AIAA 93-2117

Initial Galileo Propulsion System in-Flight Characterization

T. J. Barber
Jet Propulsion Laboratory
Pasadena, CA

F. A. Krug and B. M. Froidevaux
Deutsche Forschungsanstalt fur Luft- und Raumfahrt e.V. (DLR)
Oberpfaffenhofen, Germany

AIAA/SAE/ASME/ASEE
29th Joint Propulsion Conference and Exhibit
June 28-30, 1993 / Monterey, CA

Initial Galileo Propulsion System In-Flight Characterization

1.J. Barber*

Jet Propulsion Laboratory
California Institute of Technology
Pasadena, California

F.A. Krug •* and B.M. Froidevaux•*
Deutsche Forschungsanstalt für Luft- und Raumfahrt e.V. (DLR)
Oberpfaffenhofen, Germany

Abstract

The Galileo RetroPropulsion Module (RPM) has performed excellently throughout the first three years of mission operations. The RPM is a state-of-the-art, pressure-fed, bipropellant propulsion system, provided to NASA by the Federal Republic of Germany. Due to efficient navigation, propellant margin has substantially increased since launch, enabling extensive contingency maneuvering and the second asteroid flyby while maintaining the confidence level of successfully completing the orbital tour of the planet Jupiter beginning in 1995. The RPM has responded very well to the challenges brought about by the attempts to deploy the Galileo High Gain Antenna (HGA). No thruster thermal instabilities have been observed during any 10-N thruster maneuver through the end of 1992. RPM 10-N thruster performance has been within specification; however, the lateral thruster performance shifts have been non-negligible and remain unexplained. Nearly all Galileo 10-N thrusters are exceeding ground performance test levels by 1% to 7o/.. The pressure regulator has operated nominally throughout approximately sixteen regulator openings through the end of 1992. An RPM system health check based on helium mass calculations (helium mass budget) has demonstrated no discernible helium or propellant leakage to date.

L. Introduction

Even two years before the launch of the highly successful Voyager spacecraft to the outer planets, JPL and NASA Ames Research Center had begun work on a Jupiter orbiter and atmospheric probe mission. Originally named JOP (Jupiter Orbiter and Probe), the mission now known as Galileo was chosen as the most important new planetary mission by NASA in 1975. The threw primary science objectives of the Galileo mission are (1) to determine the physical state and chemical composition of the Jovian atmosphere, (2) to investigate the physical state and chemical composition of the Jovian satellites (primarily the four large Galilean moons), and (3) to determine the physical structure and dynamics of the Jovian magnetosphere. The Galileo mission will be unique in several respects -- the first orbiter about an outer planet (gas giant) and the first outer planet atmospheric entry probe.

The Galileo project has had quite a tortured history. Initially plannod to be launched aboard the ST S (Space T ransportation System, or space shuttle) in 1982, the mission has gone through seven major redesigns. Probably most notably, the Challenger tragedy in January, 1986 canceled the planned May 1986 launch of Galileo on a direct trajectory to Jupiter. Following Challenger, shuttle safety concerns did not allow the energetic Centaur upper stage to be placed in the shuttle payload bay. The two-stage IUS (Inertial Upper Stage) lacked the energy to inject the spacecraft into a direct, E:arth-to-Jupiter (near) Hohmann transfer orbit. 10 obtain the orbital energy necessary to get to Jupiter, Galileo would have to employ the technique of gravity assist, well-documented in the literature and used on prior planetary missions such as Mariner 10 and Voyager. The mission finally selected, a VEEGA (Venus-Earth-Earth-Gravity Assist) trajectory, called for an October 1989 launch.[1] Galileo and its two-stage I US were successfully launched October 18, 1989, and the IUS placed Galileo onto the correct heliocentric trajectory (see Figure 1 j.

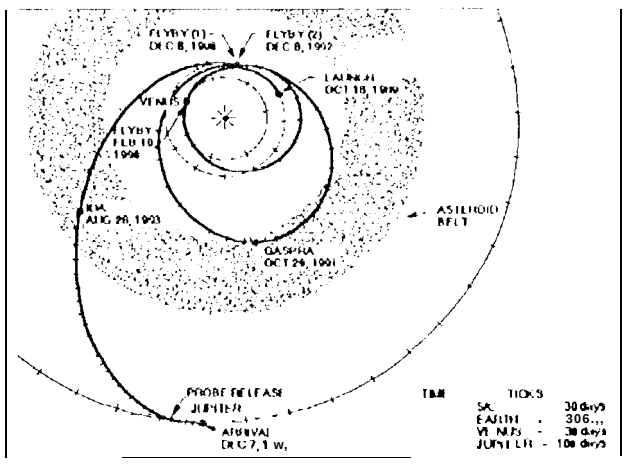

Figure 1. Galileo Heliocentric 1 rajectory

"Member Technical Staff
● *Wkwm,chafflicher Mitarbeiter bei DLR

Following IUS separation, Galileo traveled towards the sun for a Venus gravity assist on February 10, 1990, This placed the spacecraft into an orbit with aphelion slightly greater than 1 Astronomical Unit (AU). On December 8, 1990, Galileo obtained a gravity assist at Earth, placing it into an elliptical orbit about the sun with a period of exactly two years. Therefore, the Earth was positioned at the same point in space on December 8, 1992, for a second Earth gravity assist for Galileo. This finally gave Galileo the orbital energy needed to reach Jupiter.

Science opportunities for Galileo were utilized at Venus and at the Earth-Moon system. In addition, an initial reconnaissance of the main-belt asteroid 951 -Gaspra was realized with minimal propellant cost. This has high scientific value, because no main-belt asteroids had boon observed except from Earth-based observatories as points of light. Another main-bolt asteroid, 243-Ida, will be explored by Galileo in August, 1993. The Gaspra encounter was located roughly near the aphelion of the Earth-to-Earth trajectory leg, while Ida nearfy intersects the Earth-to-Jupiter path at the halfway point.

Almost two years will pass after the Ida closest approach before the next major planned mission event. In July, 1995, the atmospheric entry probe will be released from the orbiter and plummet ballistically towards Jupiter. After deflecting from an impacting trajectory with Jupiter, the orbiter will fly by the Jovian satellite 10 on Dec. 7.1995. This slows the spacecraft down and eases the propellant requirements for the Jupiter Orbit Insertion (JOI) bum, which occurs hours later near perijove (see Figure 2). At approximately the same time, the probe will enter the Jovian atmosphere, relaying its scientific data to the orbiter for transmission to the Earth (see Figure 3). Probe data return is expected for 60 to 75 minutes.

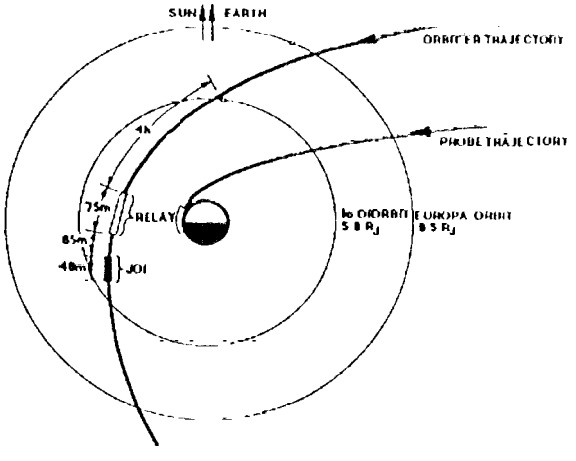

Figure 2. Galileo Jupiter Arrival Geometry

For the next twenty-three months, the orbiter will carry out scientific investigations of the Jovian "miniature solar system,'

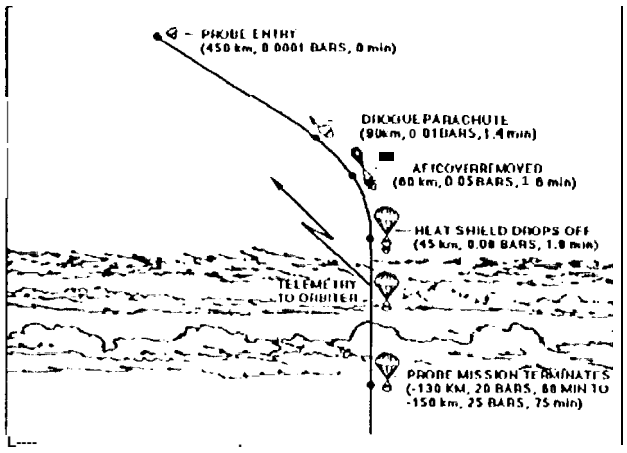

Figure 3. Galileo Probe Descent

executing at least ten orbits about Jupiter (Figure 4). Each orbit offers a close encounter with one of the four large Galilean satellites, necessary to obtain a gravity assist from that satellite to steer the path of Galileo towards the next satellite encounter. H has been shown that the amount of propellant required to perform the satellite tour in the absence of gravity assist would be thirty times greater than with gravity assist. Indeed, gravity assist makes the tour possible.[2] 1 he "petal plot" shown in F igure 4 also demonstrates that these satellite gravity assists allow the spacecraft to explore diverse regions of the near-Jupiter environment. 1 his allows the magnetosphere and, finally, the magnetotail to be explored in greater depth than ever before possible, in accord with the third main science objective. The nominal end-of-mission (E OM) is November, 1997, '

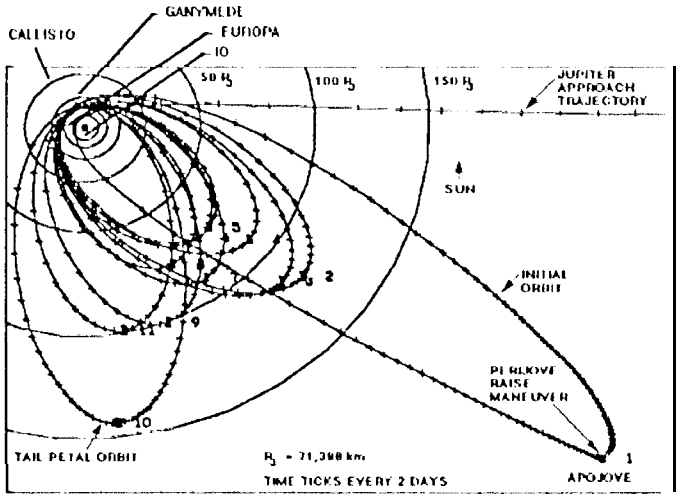

Figure 4. Galileo Jovian Orbital 1 our Petal Plot

II. The Spacecraft

Galileo was the second planetary spacecraft to be launched from the space shuttle, following the Magellan mission to Venus in May of 1989. Due to the payload bay size constraints for STS, several key portions of the Galileo spacecraft were designed to be deployed following separation from the payload bay, including the High Gain Antenna (HGA), Radioisotope Thermoelectric Generator (RTG) booms, and magnetometer boom. Therefore, the launch configuration differs somewhat from the cruise configuration.

Figure 5 shows the Galileo spacecraft nominal cruise configuration with the HGA deployed. In fact, the HGA unfurled only partially after the initial deploy command in April, 1991, leading to an asymmetric, "claw' shaped HGA. The effort to free the bound ribs of the HGA continued until the decision to use the low Gain Antenna (LGA) was made in March, 1993.

Except for this anomaly, Galileo resembles the representation in Figure 5. Galileo is a spin-stabilized, dual spin spacecraft. The spinning (spun) portion of the spacecraft contains all the fields and particles science instruments, allowing these instruments a highly desirable 4π steradian view. The stationary (despun) portion of the spacecraft contains a scan platform with imaging science instruments that require stable pointing. This design, though challenging to the designers, combines both the advantages of Voyager (three-axis stabilized) and Pioneer (spin-stabilized) in one spacecraft. In addition, the despun portion of the spacecraft holds the Jupiter atmospheric entry probe. Henceforth, the entire injected mass following IUS separation will be called the 'spacecraft," with the spacecraft being made up the "probe" and the 'orbiter.' The basic properties of the orbiter are listed in Table 1. A complete description of the Galileo spacecraft may be found in the literature.[3]

Due to the weak solar intensity at Jupiter (< 55 W/m^2 on average), the orbiter is powered using two RTGs. The total RTG power output decreases from 572 W at the beginning of the mission to 485 W on the projected mission completion date. Batteries provide electric power to the probe during its descent through the Jovian cloud decks.

The Command and Data Subsystem (CDS) of the spacecraft, with components both on the spun and despun portions, represents a significant improvement over the Voyager computer hardware. Closely tied to the CDS is the Data Memory Subsystem (DMS). The DMS tape recorder allows spacecraft science and engineering data to be recorded and returned to Earth at a later time. With the Jovian tour data (including Probe data)

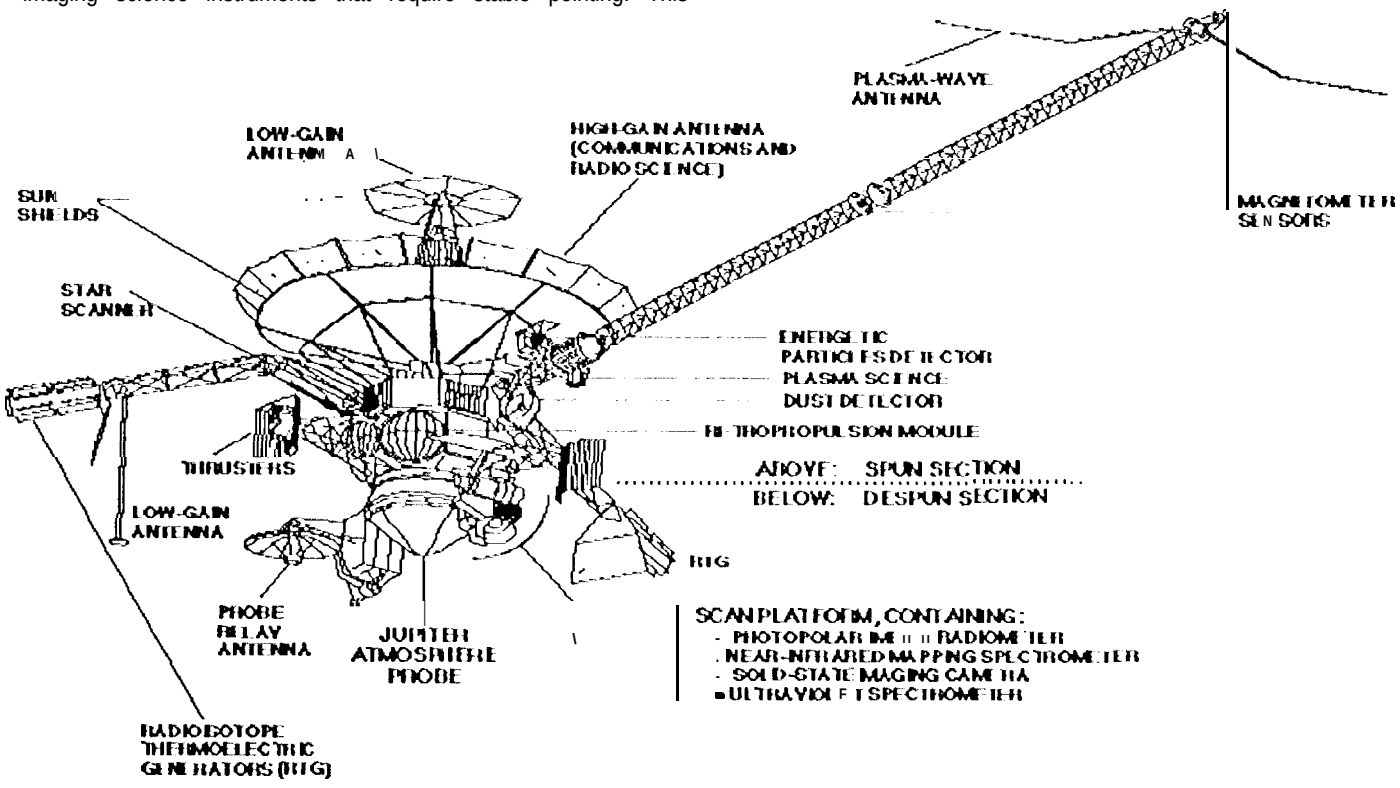

Figure 5. Galileo Spacecraft in Nominal Cruise Configuration

Table 1. Galileo Spacecraft Physical Characteristics

Parameter	Value
Launch Stack Height with Adapters	6.0 m
Launch Width	4.4 m
In-Flight Height	5.3 m
In-Flight Span (excluding Mag. Boom)	8.? m
Centerline to Magnetometer Boom Tip	11.0 m
Spacecraft Initial Mass	2561 kg
Orbiter 'Dry" Mass	1297 kg
Total Propellant Mass (Usable)	925 kg
Oxidizer Mass	571 kg
Fuel Mass	354 kg
Probe Mass	339 kg
Launch RTG Power	572 W
End-of-Mission RTG Power	485 W
Computer Resources	
-Microprocessors	22
- Memory	510 kbytes

is returned to Earth via the LGA (the current baseline plan), the DMS becomes a critical mission component,

The telecommunications subsystem utilizes X-band (HGA only) and S-band (both LGA and HGA) uplink and downlink, primarily communicating with NASA's Deep Space Network (DSN) 70 meter antennas in Goldstone, California; Madrid, Spain; and Canberra, Australia. S-band communications have been used exclusively to date, due to the HGA anomaly.

The Attitude and Articulation Control Subsystem (AACS) is responsible for maintaining the inertial pointing and spin rate for the Galileo spacecraft, as well as scan platform pointing. AACS attitude changes are accomplished by firing two of the 12 10-N bipropellant thrusters of the RetroPropulsion Module (RPM). Hence, the RPM and MCS subsystems are closely related and the RPM/AACS interface is quite critical.

Extensive on-board fault protection against a multitude of fault conditions is provided on Galileo. These fault protection algorithms are necessarily autonomous, due to long (up to almost one hour) one-way light times, the high demand for DSN tracking coverage (resulting in no tracking for days at a time), and the communication losses expected around solar conjunctions.

The Galileo scientific payload consists of 17 separate science instruments--eleven on the orbiter and six on the probe. These science instruments are of two types--fields and particles instruments and remote sensing instruments. The full Galileo scientific complement of instruments is well-matched to the ambitious Galileo objectives.

III. RPM Hardware Summary

The Galileo RPM is a bipropellant, pressure-fed propulsion system provided to NASA by the Federal Republic of Germany. It was built by MBB under contract to the FRG BMF1. The RPM provides all the propulsive capability necessary for the complex Galileo mission. A hyperbolic combination of monomethylhydrazine (MMH) and nitrogen tetroxide (NTO) is utilized for twelve trajectory correction and attitude (spin and pointing) maintenance 1O-N thrusters and one 400-N main engine used for large Galileo trajectory maneuvers. As shown in Figure 6, a set of six 1O-N thrusters is mounted in each of two thruster clusters, which extend approximately two meters from the RPM body center on opposite booms.

The RPM is a self-contained, primary load-bearing structure of the Galileo spacecraft. Principal components of the central RPM body include two helium pressurant tanks, two MMH propellant tanks, and two NTO propellant tanks, all connected with an integrating truss. Other RPM components include a pressurization and feed system, consisting of two Pressurant Control Assemblies (PCAs) on two separate equipment panels. One of these panels also carries the oxidizer feed system, called the Propellant Isolation Assembly (PIA-1), and the second includes the fuel feed system, called PIA-2. Also included is a thermal control system (for booms, thruster clusters, and the 400-N engine) consisting of thermal blankets and/or shield electrical heaters, and electrical cabling. Details on the mission requirements, design, and pre-launch performance and qualification of the RPM have been published.[4] Table 2 (reproduced from Ref. 2) lists the manufacturer and the experience with the various components of the RPM.

Figure 7 is the RF'M pressurization and feed system schematic. A great deal of redundancy has been built into the pressurization and feed system, both for shuttle safety reasons and for fault tolerance on this 8-year mission. Helium is provided to the propellant tanks via one of two redundant pressure regulators. To date, only the primary pressure regulator has hewn operated in flight. Activating the back-up operation of any RPM component. would require firing onetime pyro valves. 1 he pressurization system was designed to avoid a repetition of the regulator leakage seen on Viking. The parallel redundant regulator configuration was chosen to allow the backup regulator to be positively isolated from downstream contamination by a normally closed pyro valve. A soft seat regulator was selected to minimize sensitivity to particulate contamination. Check valves are provided to prevent MM}I and NTO vapors from reacting upstream of the propellant tanks. Since propellant vapors mixing (after permeation through check valves) was the probable cause of the Viking regulator leak, the Galileo check valves were of a unique soft seat

design which yields extremely low reverse leakage levels. To guard against possible leaking thruster valves, back-pressure relieving latch valves are provided upstream of the thrusters for reversible isolation.

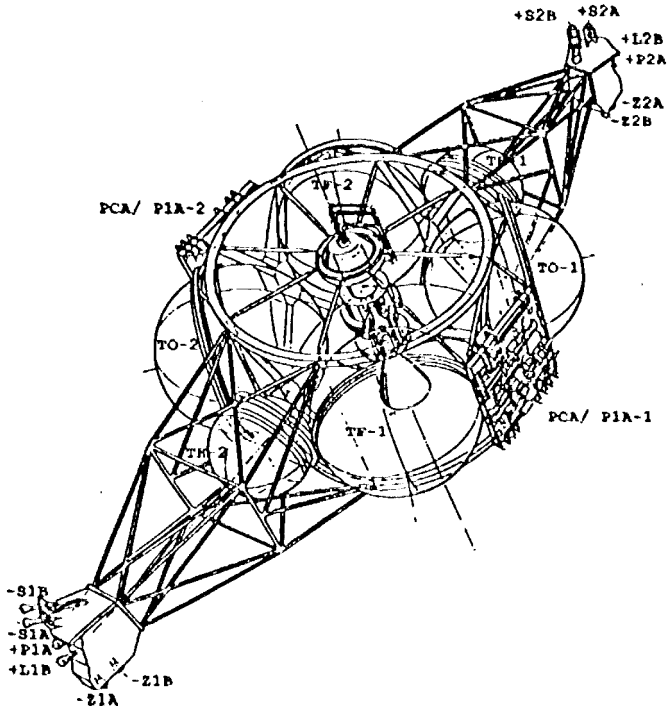

Figure 6. RPM Isometric Drawing

The design and the performance of the 10-N thruster and the 400-N engine mentioned above has been documented.[4] Figure 8 is a photo of the Galileo 1O-N thruster. For scale reference for Figure 8, the engine exit diameter is 3.5 cm. Thermal control for the Galileo 1O-N thruster is accomplished by film-cooling of the combustion chamber, MMH regenerative cooling of the engine throat, and radiative cooling of the nozzle. 10-N" thruster flight acceptance testing in earfy 1989 demonstrated some thermal instabilities in the 10-N thruster during continuous-mode operation and some hot operation during pulsed-mode operation at duty cycles with high on-time/off-time ratios.[5] High oxidizer to fuel mixture ratios and/or high total propellant mass flow rates generally aggravated the instabilities and hot operation. Therefore, to preclude these instabilities, the Galileo RPM operates the 10-N thruster in pulsed-mode only, with quite low duty cycles and with a cur-tailed operating range. Figure 9 shows the operating points of all the Galileo propulsive maneuvers superimposed on the 10-N thruster operating envelope permitted for the mission, As shown in Figure 9, the number of pulses in a single pulse train is also limited as a function of tank pressures. This mode of operation, though challenging to the engineering teams, has worked well in flight, as is evident from the excellent Galileo navigation to date.

Table 2. RPM Hardware Component Summary

RPM COMPONENT	PRO-DUCER	SOURCE/ EXPERIENCE	MAJOR CHANGES
STRUCTURE	MBB	METEOSAT	NEW DE: SIGNS
PROP. & PRESS. TANKS		SYMPHONIE	
400 N - ENGINE			NOZZLE EXTENS.
10 N - IHRUSTER			MOOG VALVE I/F. COOLING COILS
THRUSTER -VALVE	MOOG	VAR1OUS	NEW DE SIGNS
PRESS, &FEED SYSTEM	MBB		
LATCH VALVE	STERER	ELDO, RITA VARIOUS	
REGULA1OR			
CHECK VALVE			
PYRO VALVE N.O.	PYRO-NETICS	VIKING - OTHERS	NONE
PYRO VALVE N.C.			MINOR CHANGES
SERVICE VALVE			
-FILTER	VACCO		
.- PRESS. TRANSDUCER	GOULD		
RELIEF VALVE	AMETEK		NONE
TUBING	MBB "	SYMPHONIE	NEW [)ESIGN
PROPEL LANT			NO-CONTENT
THERMAL EQUIPMENT		VARIOUS	NEW DESIGNS
ELECTRICAL CABLING			

IV. Galileo 10-N Thruster Operation

The ambitious nature of the Galileo mission puts severe demands on the propulsion system for attitude maintenance,

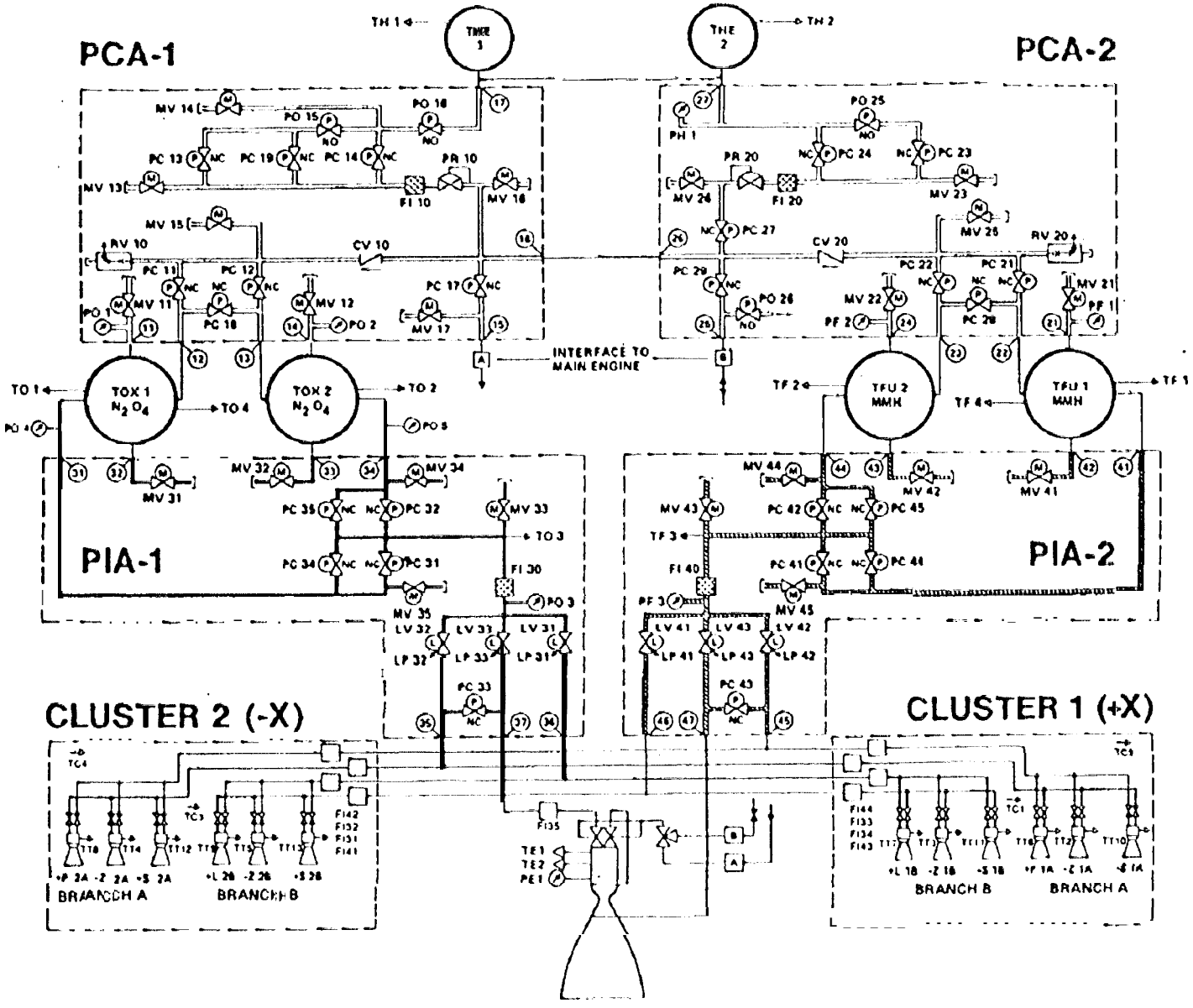

Figure 7. RPM Pressurization and Feed System Schematic

cruise 1 CMS, and large AV maneuvers--specifically, the Orbit Deflection Maneuver (ODM), Jupiter Orbit Insertion burn (JOI), and the PeriJove Raise (PJR) maneuver. Many attitude correction functions are provided for on the dual spinning Galileo. First, spin corrections to the nominal (all-spin or dual-spin) spin rate are allowed for, due to solar torques and TCM errors caused by thruster misalignments, engine performance changes, etc. In addition, large spin-rate change maneuvers (from 2.89 rpm to 10.5 rpm) are a mission requirement for probe attitude stabilization, prior to probe release, since the Jovian atmospheric entry probe has no attitude control system. Also, operation of the 400-N engine requires a minimum spin rate near 10 rpm as well, for centrifugal propellant management in the propellant tanks during the 400 N acceleration and for thrust vector control. Two sots of redundant spin-up/spin-down thrusters are used for these purposes (see Figure 10). Nominally, the S2A thruster is the primary spin-up thruster, and the S1 A is the primary spin-down thruster. The S-thrusters have been used very little through the end of 1992, since the first spin-up/spin-down demonstration capability is not scheduled until 1993.

The capability to turn the spacecraft by means of a precession maneuver is necessary for thermal reasons and for acquiring science data during the Galileo mission. Three types

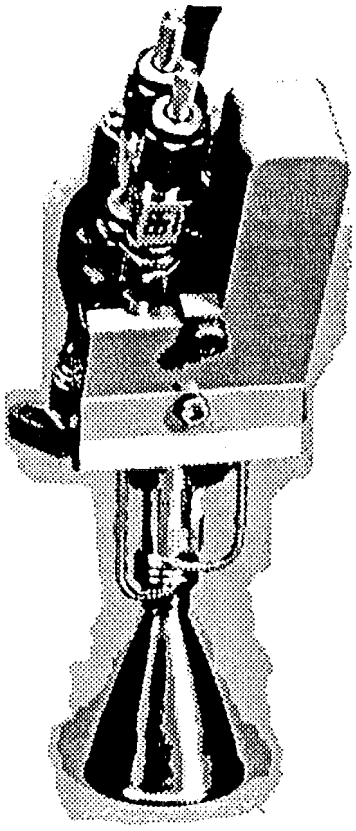

Figure 8. RPM IO-N Thruster

of precession maneuvers have been executed--Spacecraft Inertial 1 urns (S IT URNs), sun acquisitions, and HGA (pointing) corrections. SIT URNS were utilized to keep the S/C within thermal constraints due to the constantly changing off-sun angle of Galileo on the VEEGA trajectory. In particular, within solar distances of 1.0 AU, the spacecraft is required to keep its nominal spin axis within 5° of a sun-pointed attitude. An additional use for SITURNs is for "turn-burn-unwind' TCMs, which use a correctly sized SIT URN to enable the TCM to be performed in one inertial direction only. Naturally, the "unwind' portion (i.e., the turn back to the initial attitude) in such a TCM may be performed using a SITURN as well. The alternative to the turn-burn-unwind maneuver--the vector mode maneuver-will be discussed below. SITURNS maybe performed in one of two modes, either balanced or unbalanced. Balanced SITURNS are performed on the P-thrusters, which fire simultaneously once per spacecraft revolution to cancel out the net AV, as may be seen in Figure 10. Conversely, unbalanced SIT URNS may be executed by firing either the A- or B-branch Z-thrusters alternately, once per revolution. Note that in this case, a deterministic AV is added to the spacecraft,

Sun acquisitions, the third type of precession maneuver listed above, allow the spacecraft to start at any off-sun attitude and return to sun-point. This is accomplished with the AACS internally coded software control algorithms, One immediate use of the sun acquisition maneuver is evident--in case on-board fault protection on Galileo is activated, the spacecraft must be sent to a quiescent, stable and safe state until the anomaly is resolved. A sun acquisition as part of spacecraft safing satisfies all thermal control constraints, regardless of the solar distance. Sun

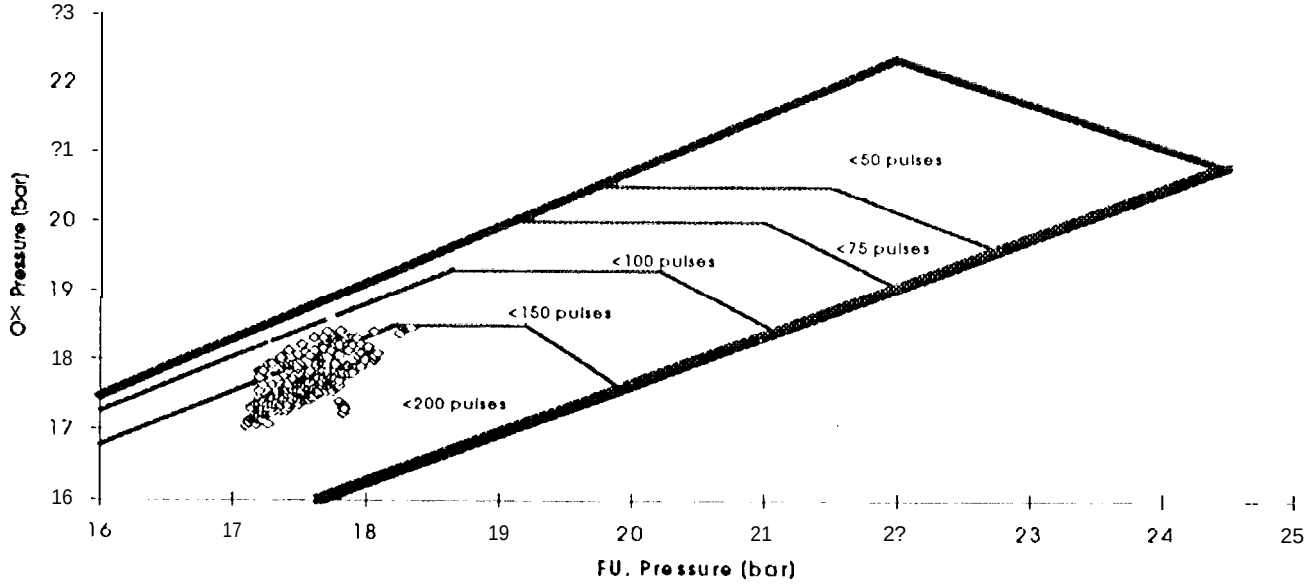

Figure 9. RPM 1O-N 1 hruster Operating Box with Flight Data

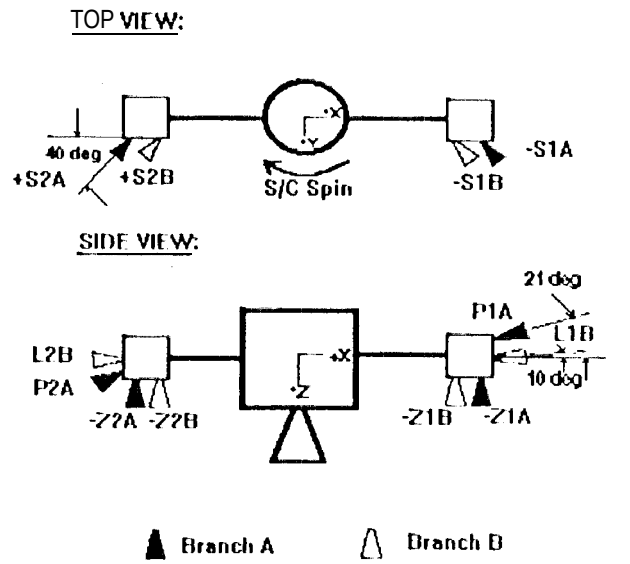

Maneuver	Operated Thrusters Primary	Backup
Attitude Control:		
-Spin-up	S2A	S2B
-Spin-down	-S1A	-S1 B
-Precession Control	P1A/ P2A	L1B/ L2B
-Unbalanced 1 urns	-Z1A/ -Z2A	-21 B/-Z2B
Trajectory Control		
-Axial AV	-21 B/-Z2B	-Z1A/ **-22A**
-Lateral AV	L1 B/ L2B	PI A/ P2A

Figure 10. RPM 1O-N Thruster Configuration

acquisitions are performed also using the P-thruster couple, but since their on-times are not individually calculated to balance their impulse, a small AV is imparted on the S/C during a sun acquisition.

Finally, HGA (or pointing) corrections allow the high gain antenna to be pointed towards the Earth, within the tight tolerances dictated by X-band telecommunications. In addition, pointing corrections are necessary during TCMS because thruster misalignments or performance changes can cause the spacecraft to process sufficiently such that the AACS star set chosen for the TCM (for accurate attitude reference) is no longer viable. These, too, are performed on the P-thrusters in a quasi-balanced mode.

Many relatively small TCMS (AV < 40 m/s) are necessary throughout the VEEGA cruise and Jovian orbital tour. These maneuvers are basically of two types-deterministic and statistical. Relatively small deterministic maneuvers during the VEEGA trajectory include TCM-1 (which removed the nominal launch bias of 17 m/s), TCM-4 through 1 CM-7 (which targeted to the first Earth encounter in December 1990), TCM-1 O (which targeted to the Gaspra flyby in October, 1991), TCM-14 through TCM-16 (which targeted successively closer to the second Earth flyby in December, 1992), TCM-19 (which targets to the Ida flyby in August, 1993), and T CM-22 (which targets for the probe release trajectory). The remaining TCMS are statistical (i.e., nominally zero), but are provided for to 'clean up" execution errors of the deterministic maneuvers as well as to compensate for interplanetary orbit perturbations. In addition, the statistical T CMS prior to the Gaspra and Ida flybys are positioned so as to take full advantage of the technique of optical navigation to better determine the position of these asteroids for a successful scientific reconnaissance.

Due to the various S/C pointing constraints mentioned above, the capability to perform these relatively small TCMs is provided in both the ± Z-direction (along the S/C spin axis) and in the lateral direction. A 'vector mode" maneuver represents one way, then, to perform a given maneuver. In this case, the S/C's attitude is kept steady throughout the maneuver and the correct amount of AV is achieved by splitting the AV into the correct amount of lateral and (±) axial thruster firing. Alternatively, such a maneuver may be accomplished by first processing to the appropriate attitude ("turn"), firing along either the lateral or ± Z-direction ("burn"), and then processing back (*unwind') to the original attitude via a SIT URN or sun acquisition Such turn-burn-unwind maneuvers can offer propellant savings when compared with the analogous vector mode maneuver depending on AV magnitude and direction .

Lateral thruster segments have been employed in every Galileo TCM through the end of 1992. In this operating mode, the L1B and L2B thrusters fire alternatively, once per revolution. The thruster on-times are set individually such that the net torque on the spacecraft is zero. However, a small AV component is generated along the +Z axis each time a lateral maneuver is executed. Since the inertial firing position may be specified for a lateral maneuver, a lateral maneuver may be executed in any lateral direction perpendicular to the spin axis.

Two types of axial maneuvers have been executed by Galileo. The most common is a PUL7(-Z) maneuver, which imparts a velocity increment to the spacecraft in the -Z direction. Unlike the unbalanced turn mode, this type of maneuver fires each of two opposite Z-thrusters simultaneously twice per revolution, canceling the net torque. Another type of axial maneuver is the POSZ(+ Z) maneuver, which increases the spacecraft velocity in the +Z direction. As may be seen in Figure 10, only the PIA and the L1 B thrusters have a component in the spacecraft +Z direction. A POSZ maneuver does not cause spacecraft precession, since the PIA thruster is fired twice per revolution applying opposite

torques. Since the thrust component of the PI A thruster in the +Z direction is not large (sin 210), this type of maneuver is not very efficient and is generally avoided, if possible, even by occasionally biasing the trajectory slightly.

1 here is one common Galileo propulsive activity that is performed to maintain the RPM. At least every twenty-three days (a number arrived at through theoretical modeling), all RPM 1O-N thrusters are operated for a minimum on-time of 1.2 seconds. These so called thruster 'flushes' are necessary to limit the build-up of products from the interaction of NTO with some small stainless steel components (nearly all hardware in contact with NTO is made of a titanium alloy, which resists such corrosion). These products may accumulate to the point that they could clog filters or small flow passages.[6] These flushing maneuvers are designed to give the spacecraft as little AV as possible, but it is clear that the AV in the -Z direction from all the Z-thrusters will not cancel. Navigation has accepted this AV in the -Z direction, since it is of small magnitude (average of 18.2 mm/s for the total of all four Z-thrusters) and, more importantly, because it is repeatable (typical deviation from the mean is ±0.2 mm/s) and in a known direction. These thruster flushes have little operational impact on the Galileo mission, since trajectory correction is not adversely affected and because the total propellant cost of the thruster flushes throughout the entire mission is only ≈7 kg (<1% of the total usable propellant). One benefit of the thruster flushes is the ability to analyze thruster performance vs. ground-test levels for little used engines like the S-thrusters.

1 he operating modes of the Galileo 10-N thrusters are summarized in Table 3. This table describes the allowable duty cycles for the maneuver types fisted above, given the restrictions following the final acceptance testing in early 1989. It should be stated here that, to the best of our knowledge, no thermal instabilities have occurred in any Galileo 1O-N thruster during in-flight operation through the end of 1992. However, a minor thermal instability was observed on the SIA thruster during the spin-down maneuver in March, 1993. 1 his anomalous behavior is currently being analyzed.

V. Galileo RPM Telemetry Measurements

The Galileo RPM Analysis Team is afforded good visibility into the in-flight operation of the RPM from a variety of telemetry measurements. Measurements are provided for the propellant and pressurant tank pressures and temperatures, cluster temperatures, 10-N thruster temperatures, and 400-N engine temperature and chamber pressure. In addition, AACS telemetry is provided to RPM for the calculation of the 1O-N thruster firing history; namely, the number of executed thruster pulses and the accumulated thruster on-time, The health and safety of the RPM is determined both from the telemetry measurements described above and from parameters derived from RPM and other telemetry.

Table 3. 1O-N Thruster Operation Limits and Extreme Values

MANEUVER TYPE	Thruster Duty Cycle		Max. number of pulses per thruster and maneuver segment	
	On-time (max.) [s]	Off-time (min.) [s]	Performed in flight	Allowed by flight rule
SPIN CORRECT (A or B)	1.34	8.18	2	5
SPIN-UP/DOWN (A or B)	1.30	3.90	0	350
BAL TURN (A)	1.06	17.98	223	500
UNBAL TURN (A)	0.83	18.21	31	500
SUN ACQ. (A)	1.39	19.35	287	500
HGA POINTING (A)	1,19	17.85	3	500
LAT TCM (D)	2.62 1.32	16.42 17.72	24 150	31 500
PULZ TCM (B) (A)	0.94 0.94	8.58 8.58	166 96	500 500
POSZ TCM [A]	1.14 0.94	8.38 8.58	62 172	100 500

Multiple pressure telemetry channels are provided for the NTO and MMH tankage systems, while the helium tanks are instrumented with just one pressure transducer. Three telemetry measurements are averaged to calculate both the mean oxidizer and fuel pressures. The telemetry channels P_{O1} and P_{02} measure the gas-side pressure in the first and second oxidizer tanks, respectively; P_{F1} and P_{F2} are used similarly for the two fuel tanks. The two oxidizer tanks, as well as the two fuel tanks, are connected together via a feed line and a pressure measurement is taken in this line (termed P_{O3} and P_{F3} for the oxidizer and fuel lines, respectively). Since the tanks are physically connected, ideally all three telemetry channels should read identically, except during large pressure transients (large maneuvers), in which the line pressure is slightly below the tank pressure. By investigating the relative difference between any two of the three redundant pressure telemetry channels over time, possible relative drifts may be determined. While the difference $P_{O2} - P_{O3}$ has remained stable, the other two oxidizer differences (P_{O3} - PO, and PO, - P_{02}) have not. The simplest explanation commensurate with

these facts is a drift of the PO, pressure transducer with time of +0.0755 bar/year. This is a drift of nearly one DN (Data Number) per year, where one DN is defined to be the smallest digital unit in the analog-to-digital conversion of the pressure transducer signal. The pressure range is divided into 258 DN in these 8-bit telemetry channels. This drift has to be taken into account whenever a value for oxidizer pressure is used--for example, in the design of 1O-N thruster maneuvers, the back-up design of (the nominally accelerometer controlled) 400-N engine bums, the estimates of propellant consumption, and the determination of propellant mixture ratio. A similar analysis was performed for the three fuel pressure transducers to determine their relative drift rates. Maximum drift rate of P_{F1} was determined to be at least a factor of four smaller than the inferred PO, drift rate. The PO, drift may be - due to random electronic parts drift. Such phenomena are not unanticipated; similar effects were noted in the Voyager monopropellant hydrazine tank pressure transducers.

The oxidizer and fuel tank pressures are functions of many spacecraft variables, including off-sun angle, solar distance, power margin, propellant expulsion, and regulator state. Power margin affects tank pressures because the power subsystem shunt radiators are bonded to the RPM tanks. The first three variables influence the propellant tank pressures indirectly through changes in RPM propellant tank temperatures; the final two variables affect tank pressure directly. The primary factors that have influenced the RPM tank pressures to date are propellant expulsion and regulator operation during large TCMS in addition to large solar heat input at large off-sun angles and diminished solar distances. Considerable effort has been expended to control tank pressures by manipulating the spacecraft power margin.

The single pressure transducer measuring helium pressure (P_{H1}) has a resolution about ten times more coarse than the NTO and MMH tank pressure telemetry. T his is because the range of data numbers (O-255 DN) is allocated to a pressure range ton times larger than the typical propellant tank pressure range. T his coarse resolution makes accurate determination of the amount of helium in the pressurant tanks difficult. This will be discussed further below, in the context of a computed helium budget. The helium tank pressure depends on the same variables as the propellant tank pressures do, with the exception that propellant expulsion only indirectly influences the pressure through the pressure regulator operation.

There is no telemetry to indicate the chamber pressures within the 10-N thrusters. However, the 400-N engine is instrumented with such a chamber pressure measurement. This will allow more complete characterization of the 400-N engine performance during ODM, JOI, and PJR. Since the 400-N engine chamber pressure transducer has always indicated a perfect vacuum as expected, within DN uncertainties, no further mention of this telemetry channel is necessary.

As for the pressure measurements, multiple telemetry channels are used to determine the average oxidizer and fuel tank temperatures as well. 1 he helium temperature is only used to calculate the helium content in the pressurant tanks. For that purpose, a mean helium tank temperature calculated by averaging the individual sensor output from each of the two helium tanks will suffice,

As alluded to above, RPM tank temperatures depend on off-sun angle, solar distance, and power margin (since excess RTG power is dissipated in a shunt heater located on the RPM central body structure). Because off-sun angles and solar distance are pre-determined, the power margin is adjusted to control RPM tank temperatures (and pressures). The strongest variations in the tank temperature correspond to HGA anomaly activities. While the attempts to deploy the HGA have challenged the propellant tank pressure management strategies, they have also allowed a much more complete thermal characterization of the RPM than would have otherwise been possible.

Four telemetry channels are provided for measuring the thruster cluster temperatures on the Galileo spacecraft, two on each cluster, These cluster sensors are used to thermally characterize the RPM cluster environment, particularly during 1O-N thruster firings. During a long propulsive maneuver, cluster temperatures may approach 40°C, starting from an initial temperature of around 20°C. In steady-state firing ground tests, the propellant entered the 10-N injector basically near the propellant tank temperature of 20°C. However, in a pulsed firing mode, it was found in flight that the 1O-N thrust level during a maneuver segment seemed to decrease as the cluster temperatures increased. This could only be explained by modeling (in maneuver reconstruction) propellant temperatures to be the cluster temperatures. This makes sense intuitively, considering the long dwell times of the propellant in the 1O-N thruster valve (cluster) region of about 20 seconds before expulsion and the MMH heat input from the regenerative cooling loop. However, it was unanticipated before experience was gained in pulsed mode 1O-N thruster operation.

Each cluster is heated by eight Radioisotope Heating Units (RHUs) each generating about one watt. In addition, there are two electrical heaters per cluster which allow further control of the cluster temperature. T he heater states have been varied in the past during HGA thermal turns to large off-sun attitudes, depending on solar distance. In addition to depending on off-sun angle, solar distance, heater state, and thruster firing state, cluster temperatures are actually weak functions of the RPM central body temperature, as Figure 11 demonstrates. Although the correlation is not strong, this result was unexpected from Solar Thermal Vacuum (STV) ground testing . Figure 11 comprises temperature data from 1992 which includes off-sun angles of <24° and solar distances from 0.98 AU to 2.27 AU.

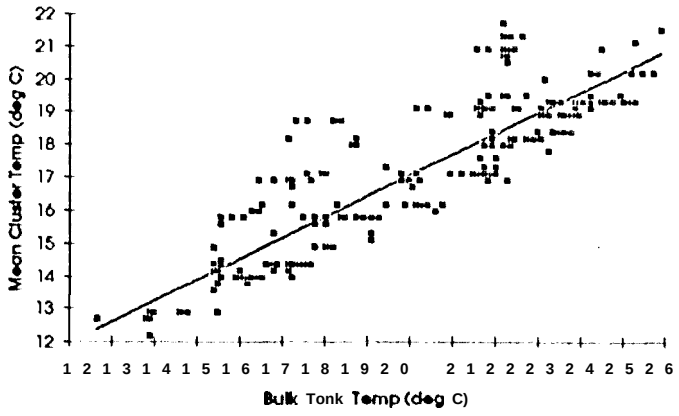

Figure 11, RPM Central Body/ Thruster Cluster Thermal Coupling

The 400-N engine temperature is determined by two separate transducers. They are mounted to the outside of the 400-N engine chamber. Primarily due to thermal shielding by the probe, these temperatures stay almost constant at 57 to 58°C with the primary of the two available 400-N electrical heaters on. However, the 400-N engine temperature is regulated actively by a temperature monitor control algorithm. In particular, if the temperature indicated by 400-N engine temperature sensor increases beyond approximately 60°C, both heaters are turned off and 400-N engine heater cycling begins. To prevent the 400-N engine from getting too cold, the primary heater is turned back on when the 400-N engine temperature falls below 5°C. In case the primary heater has-failed, the fault protection automatically turns on the secondary heaters if the temperature drops to O°C. This heater cycling has beon documented by the RPM, and Figure 12 shows an example cycling profile. The period of this cycling is approximately 33 hours. Figure 12 demonstrates that the 400-N engine temperature control algorithm has worked well in flight.

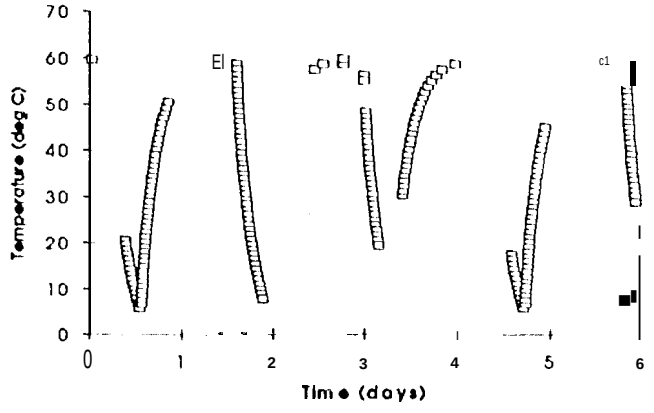

Figure 12. RPM 400-N Engine Heater Cycling

Thruster temperature transducers were added to all 1O-N thrusters shorty before launch. They were mounted externally to the firing chamber to help further characterize 10-N thruster in-flight performance. Although the temperatures measured by these sensors are not a typical propulsion system variable (such as chamber or throat temperature, as they are located above the cooling coils in Fig. 8), they should correlate well with changes in thruster operation, if with reduced clarity. Figure 13 shows a typical firing thruster sensor temperature profile during a large maneuver. Various aspects are evident from the figure: the small rise time, the relative constancy at equilibrium (with a slight ramp up due to the accumulation of heat in the cluster which drives the thruster temperature up), the "soakback" at the end of the maneuver and the radiative cool-down curve. These sensors are only used for detecting possible anomalies and trends.

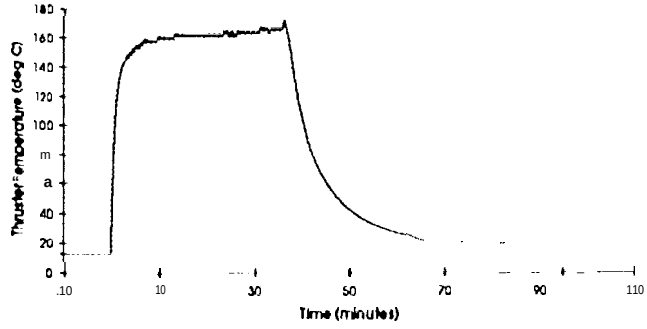

Figure 13. RPM 1O-N Thruster Temperature Profile

To date, four out of the twelve thruster temperature transducers have failed open circuit. Since they were not originally required in flight, but were added to the spacecraft shortly before launch, the sensors and their mounting were never flight qualified. The first thruster temperature sensor failure occurred during TCM-1, 23 days after launch. It was on the 21A thruster, which was being used with the 22A thruster to impart a negative-Z direction (PULZ) velocity change to the spacecraft. Figure 14 details the 21A thruster temperature sensor failure. Since the output of the transducer jumped from nominal to an open circuit value (255 DN, approximately 600°C) within one telemetry update (and cluster temperatures were nominal as well), it seemed unlikely that there was a thermal 'runaway' of the thruster. Following the end of the maneuver, the transducer suddenly returned to a reading in agreement with expectations. It appeared to be working correctly until the next maneuver utilizing that thruster. Another open circuit failure followed during that maneuver. This cycle repeated a few times, until finally the Z1A thruster temperature sensor failed open circuit for the final time. This failure behavior was duplicated exactly for the other three thruster temperature transducer failures (the L2B, PI A, and P2A thruster temperature sensors). Given the data, it appears likely that the thermal stresses and strains associated with the maneuver fractured a lead or sensor wire on

the temperature transducer. Once the maneuver was completed and the transducer had cooled down, the severed wires would again make contact and form a circuit, This cycle continued until eventually the severed wires no longer contacted each other, even during thruster non-firing periods. The failure of these sensors has reduced visibility into the thruster behavior but the cluster temperatures allow the detection of any anomalous behavior.

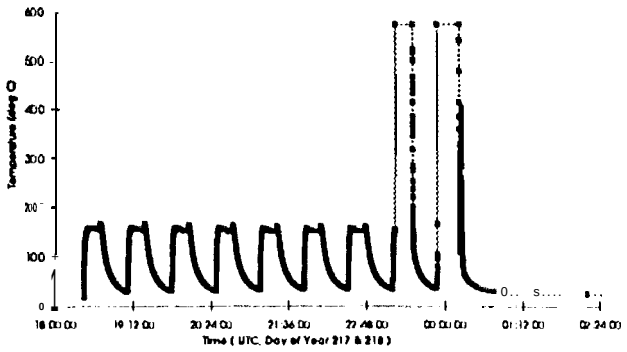

Figure 14. RPM 21A Thruster Temperature Sensor Failure

The correct execution of a commanded TCM is verified through AACS telemetry measurements. The individual thruster firing time (in steps of 1/90 seconds, called "counts") and the total number of ail thruster actuations may be obtained in this manner, More information on these telemetry channels will be provided below, in the section concerning spacecraft consumables.

VI. HGA Deployment Activity Summary

On April 11, 1991, the initial deployment of the Galileo HGA was unsuccessful. It was eventually determined that three of the eighteen graphite-epoxy ribs were most likely restrained at the central tower probably due to the frictional binding of guiding pins in their receptacles, resulting in a partially unfurled, asymmetric HGA. In addition to the challenges associated with flying the VEEGA trajectory, the extensive efforts to deploy the HGA have brought with it special challenges to the RPM mission operations team and the propulsion system itself. A summary of the initial HGA deployment attempts has been documented.[7]

Shortly after the initial deployment attempt, it was hypothesized that the pins were frictionally bound to the central tower due to differential thermal expansion between the central tower and the ribs. Therefore, the first identified contingency action was the thermal cycling of the HGA. The first indications called for a warming of the stainless steel central tower to lengthen the tower with thermal strain (the graphite-epoxy ribs have nearly zero coefficient of thermal expansion). To enable this tower heating, the spacecraft, normally approximately sun-pointed, was turned to a 45° off-sun attitude for nearly 48 hours. This so called HGA Warming Turn 1 was performed in May, 1991, at a solar distance of 1.56 AU. Such large off-sun angles were not anticipated during the Galileo mission, at least so close to the sun, and as such, spacecraft thermal health and safety had to be very carefully managed. The spacecraft performed very well during this thermally stressful time period, the RPM included, The warming turn provided the RPM subsystem with a perturbation to the normally quiescent thermal state of the subsystem. This was primarily due to increased solar input to the 1O-N thrusters, clusters, and propellant and pressurant tanks at this large off-sun attitude. Propellant and pressurant tank temperatures (and hence, pressures) rose steadily throughout the warming period. However, the increases were slight due the large thermal inertia of tho RPM central body. Propellant and pressurant tank temperatures increased by 2 to 3°C (=1%), respectively, and the propellant and pressurant tank pressures increased by only 0,2 bar and 2.0 bar, respective y (also =1%). Longer durations at the 45° off-sun attitude would have eventually increased the tank temperatures and pressures beyond flight limits. The time at a 45° off-sun attitude was limited by non-RPM hardware as well. However, this did not constrain the maneuver, since the HGA central towor heating time constant is sufficiently short such that thermal equilibrium is obtained within 48 hours. Cluster and thruster temperatures increased more significantly, typically by 15 to 20°C before the return to a sun-pointed attitude. Simple exponential curve fits were determined for the cluster and thruster temperature profiles following the SITURN to a 45° off-sun attitude. The characteristic time constant for the solar heating was nearfy 10 hours for most of the measurements. Therefore, thermal equilibrium was basically obtained for the thruster and cluster temperatures by the time the 45° sun acquisition was performed. Since the propellant temperatures at the injector inlet in pulsed mode operation do not remain at the tank temperature, but rather approach the cluster temperatures, there was some concern about the cluster temperatures during the sun acquisition maneuver. In particular, a sun acquisition utilizes the P-thrusters, and the 1 c2 cluster temperature sensor may be taken as roughly equal to the PIA propellant inlet temperature. Operation of the Galileo 1O-N thrusters above a propellant inlet temperature of 60°C is prohibited, since at 68°C the vapor pressure of NTO is 7 bar , the same as the 10-N thruster chamber pressure, so that two-phase oxidizer flow in the injectors can be expected at such elevated temperatures. The maximum T_{C2} reading (just prior to the completion of the sun acquisition) was near 46°C, comfortably below the operating limit of 60°C. Unfortunately, despite excellent spacecraft health during the maneuver, the HGA remained bound.

Following this HGA warming period, further analysis determined that tlGA central tower cooling was a more likely means by which to relieve the pin friction. Cooling the HGA to a sufficient level required off-sun angles of at least 165°. This orientation, nearly anti-sun-pointed, precluded downlink over the primary low gain antenna (LGA-1). Rather, a rear-looking low gain

antenna (LGA-2, added to the spacecraft due to sun-pointing requirements during the near-sun portions of the VEEGA trajectory) was utilized. The first HGA Cooling Turn was performed July, 1991, to an off-sun attitude of 165° for ≈36 hours. Although there were many similarities to warming maneuvers, the 165° off-sun attitude presented the RPM with some new concerns. The largest difference was manifested in the cluster and Z-thruster temperatures. Due to plume impingement requirements for the Z-thrusters, there can be no sun-shade or plume shield below the Z-thrusters. Therefore, the first HGA cooling period allowed direct solar illumination into the nozzles of all four 10-N Z-thrusters, increasing their temperature by nearly 30 "C during the 36 hours at attitude. Also, cluster temperature increases were higher than in the first HGA warming interval, rising 20 to 30°C. This was even with a modification to the cluster heater state while at attitude. The maximum cluster temperature throughout the activity was nearly 53°C on T_{C2} at the end of the sun acquisition maneuver, only 7°C below the specified limit. And this was at a solar distance of 1.84 AU. Clearly, anti-sun turns nearer to the sun could have been a problem. As it turned out, the atmospheric entry probe relay antenna on the orbiter was even more sensitive to anti-sun attitudes at low solar distances, so the RPM cluster temperature was not the limiting factor. In summary, the RPM had again performed excellently in an unanticipated thermal state.

The effort to deploy the HGA continued. Since Galileo was still traveling away from the sun, more HGA cooling could be obtained with subsequent 165° off-sun turns. Two more HGA Cooling Turns were performed, one before and one after the Gaspra encounter in October, 1991. Again, the RPM hardware was nominal throughout the period, The second HGA Cooling Turn was performed in August of 1991 at solar distance of 1.97 AU; the third was executed December of 19912.26 AU from the sun. Galileo would not be further from the sun until well into 1993, after the final Earth gravity assist. A special challenge was levied on the spacecraft team for the third cooling turn--it was necessary to perform most of the maneuver "in the blind." In particular, there would be no downlink at the 165° off-sun attitude and telemetry would not be reacquired until the sun acquisition returning the spacecraft to sun-point was nearly complete. All spacecraft subsystems performed well during this period.

Before the third HGA Cooling period, the HGA Anomaly Team had determined that the frictionally bound pins might loosen if they could be 'walked out" with alternate warming and cooling periods. Therefore, a series of four warming/cooling cycles were performed on the spacecraft between January and July of 1992. Although no movement of the HGA was determined, the RPM subsystem performed nominally throughout the periods with strong thermal transients.

During the thermal cycling campaign, the HGA anomaly team developed more aggressive means to deploy the HGA. 1"0 begin, it was decided to activate the Duaf Drive Actuator (DDA) assembly again as a diagnostic. This DDA1 sequence of DDA activity demonstrated that motors were working properly (at stall). No more mention of DDA1 will be made, since it was quiescent with respect to the RPM. Following this, during the DDA2 sequence, two pulses of 1.8 second duration were executed on the deploy motors; one at a cold HGA temperature, the other aHer ≈28 hours at an off -sun attitudeof310 and a solar distance of 1.80 AU. In addition, LGA-2 was retracted during this mini-sequence (this activity had been planned all along). The dynamics of the retraction process were examined to see if they could be useful for deploying the HGA. Although no significant ball-screw rotation occurred during DDA2, the tests did determine that the motors were still working nominally at stall. Most notably to the RPM Analysis Team, the turn toa310 off-sun attitude was performed in an unbalanced mode using the A-branch Z-thrusters, which allowed large savings in propellant consumption. Just one small (=7°) unbalanced turn had been performed prior to this. The A-branch Z-thruster performance during these maneuvers will be discussed below.

Since Galileo was traveling inbound towards its second Earth flyby, the prospects for tower and DDA heating were improving. The DDA3 activity was designed to be quite similar to DDA2, with the following exceptions: the LGA-2 state was not altered, the off-sun attitude was increased to 45°, and the solar distance had decreased to 1.6 AU. This turn was executed in balanced mode using the P-thrusters. At such low solar distances (<1.8 AU) use of the Z-thrusters is minimized because using them could conceivably trigger a fault in the propulsion drive electronics (referred to as a "stuck-open Z-thruster") that could precess the spacecraft to an off-sun attitude that would adversely illuminate the Radio Relay Hardware (RRH), the future communication link from the orbiter to the probe. Since the off-sun attitude, angle and duration and the solar distance were similar for DDA3 and HGA Warming Turn #1, there were no outstanding RPM thermal concerns for the DDA3 activity. However, further DDA activities at increased solar intensities would have again placed the RPM in uncharted territory.

The HGA Anomaly Team had determined that "hammering"--pulsing the DDA assembly repeatedly--would increase the drive torque over a steady-state actuation. Furthermore, the torque would also increase as the DDA assembly and surrounding hardware became warmer. An extensive hammer sequence was envisioned near Galileo's last perihelion, at a solar distance of one AU just following the Earth-2 flyby. This activity would not be undertaken without a hammer characterization test (DDA4). DDA4 was performed at a solar distance of 1.3 AU, and consisted of a balanced turn to 45° off sun for 48 hours, followed by a sun acquisition. At attitude, 10 DDA pulses were executed just before the sun acquisition, at a frequency of 1,25 Hz and a duty cycle of 33%. The spacecraft performed well throughout the

entire period, and some ball screw" rotation resulted. 1 his enabled an aggressive DDA5 plan to be implemented. Thermal modeling by the RPM Analysis Team and the Temperature Control Team had determined that all RPM hardware would be safe during this large perturbation to the spacecraft thermal state. In particular, the RPM Team predicted that cluster temperatures would not approach the 60°C limit, even at 1 AU (as long as the cluster heater settings were adjusted). The cluster temperatures during DDA4 were as expected.

Table 4 represents an RPM summary of all HGA anomaly activity through end-of-year 1992, including DDA2 through DDA4. The question marks in Table 4 correspond to a lack of telemetry at the off-sun attitude, due to downlink limitations. Maximum cluster temperatures in Table 4 are obtained just prior to sun acquisition completion. During these HGA recovery activities, a total of 45 kilograms of propellant were used to maneuver the spacecraft to the desired off-sun attitudes for HGA thermal variations. However, despite this unanticipated propellant cost, the projected End-Of-Mission (EOM) propellant remaining (propellant margin) is now -3 kg, vs. -58 kg at launch. This is due to improvements in optimization of the placement and magnitude of TCMs, excellent navigation, and the selection of a very low AV cost orbital tour. Incidentally, the propellant margin quoted above is a ninetieth percentile figure for ten targeted Galilean satellite encounters and includes significant statistical components. 10 summarize, the RPM performed excellently in response to the challenges levied by all HGA deployment activity periods,

VII. RPM Consumable Summary

The primary RPM consumables are propellant (MMH and NTO) and latch and thruster valve cycles. 1 he usable propellant remaining is probably the most critical spacecraft consumable since it is likely to be the life-limiting resource for the mission (although RTG power output decay and accumulated radiation damage are contenders as well). In addition, the accumulated latch and thruster valve cycles are critical consumables.

Thruster models have been developed based on ground test data. From these models, estimates of the oxidizer and fuel consumption during a given maneuver may be obtained. Specifically, the oxidizer and fuel tank pressures, maneuver on-time, and propellant (cluster) temperatures are entered as input. Output from the model includes the specific impulse (Isp), total mass flow, engine thrust, mixture ratio, and NTO and MMH consumed during the maneuver. The RPM Analysis Team keeps a running tabulation of the propellant consumed throughout the mission. Figure 15 displays the usable total propellant on the Galileo spacecraft as a function of time through EOY 1992. Nearly all of the propellant to date has been spent during TCMS and HGA recovery activities. Particularly large propellant costs were incurred during TCM-1, TCM-4A, 1 CM-14, and all HGA Cooling Turns. However, as mentioned previously, the propellant margin has improved substantially since launch. Further improvements are expected with the use of unbalanced turns for spacecraft precession maneuvers once Galileo is permanently outside of 1.8 AU (after April, 1993). This mode of operation will save significant amounts of propellant during the remainder of the

Table 4. HGA Deployment Attempts Summary with respect to RPM

				OFF-SUN		+X Cluster			-X Cluster		
MANEUVER	DATE	TANK PROP, TEMP. (c")	SOLAR DIST. (AU)	ANGLE (")	DUR (HR)	+X-HTR (w)	TC1 ("c)	TC2 ("c)	-X HTR (w)	TC3 ("c)	TC4 ("c)
WT #1	20 MAY-91	23.2	1.57	45	48	2	33.2	37.7	3	29.1	31.0
CT #1	IAN-IL-91	24.1	1,84	165	32	0	38.2	42.0	0	33.6	34.2
CT #2	13-AUG-91	20.1	1.89	165	50	0	33.3	37.7	0	28.0	30.1
CT#3	13-DEC-91	16.3	226	165	50	0	?	?	2	?	?
WT #4	9 JAN 92	19.0	227	45	48	2	24.5	27.2	3	20.8	23.8
CT #4	4-FEB-92	16.2	2 26	1&5	50	0	?	?	2	?	?
WT #5	17-FE B-92	18.2	225	45	48	2	24.5	27.2	3	20.8	23.8
CT #5	2-MAR-92	15.3	2.24	165	50	0	?	?	2	?	?
WT #6	19 MAR-92	18.4	221	45	48	2	?	?	3	?	?
CT #6	13-APR-92	15.2	2.16	165	50	0	?	?	2	?	?
WT #6A	29 JUN 92	17.8	1.90	45	48	2	26.9	31.4	3	23.2	25.8
CT #6A	6-JUL-92	17.9	1,88	165	50	0	?	?	2	?	?
DDA2	2t-JUL-92	18.3	1,81	31	24	2	221	25.1	3	18.4	19,6
DDA3	8-SEP-92	23.1	1.54	45	28	2	341	37.7	3	23.2	322
DDA4	12-OCT-92	23.2	1,33	45	48	0	27.7	31.4	2	29.6	322

mission, since the Z-thrusters are nearly three times more fuel efficient for performing a spacecraft precession. Also, using the Z-thrusters for spacecraft turns will reduce P-thruster pulse cycles. From the propellant consumption data, the average mixture ratio of all 1O-N thrusters through the end of 1992 is 1,53. However, recent test data indicates that the mixture ratios as modeled by the RPM Analysis Team may have a 4% overprediction.[8] This may lead to larger NTO residuals than expected. The estimate of the mixture ratio in a bipropellant system could have important consequences for the EOM propellant residuals. However, these are small compared to the uncertainties in propellant consumption for Galileo.

The RPM Analysis Team is also the cognizant group for - latch and thruster valve cycles. Latch valves are actuated once for each separate propulsive event, such as a TCM segment, SITURN, spin or HGA correct, etc. The limit on latch valve cycles is 4000 per each of the A and B thruster branches. As of End-Of-Year (EOY) 1992, there were 687 cycles (1 7.2% of lifetime) on the A-branch oxidizer and fuel latch valves, and 377 cycles (9.4% of lifetime) on the B-branch latch valves. Many of the B-branch thruster latch valve cycles (≈80%) were incurred during thruster flushing maneuvers. However, the expected cost of future thruster flushing maneuvers has been accounted for, and it appears that latch valve cycles are not a mission-limiting consumable.

Thruster valve cycles are more critical. Table 5 shows the executed number of thruster pulses for each 10-N thruster as of EOY 1992. The thruster pulse limit is currently 23,000 pulses per thruster. Table 5 shows the current percentage of lifetime that has been expended, Although it appears that the L-thrusters may be a life-limiting concern, their frequent use during the VEEGA trajectory was forecasted. However, the P-thrusters have been used more extensively than planned due to HGA anomaly activities. If the HGA were to deploy, many P-thruster pulses will be executed to maintain tight pointing towards the Earth in order to allow communication over the narrow X-band beam of the HGA.

Since the PIA thruster is also used in POSZ TCMs, it is probably the most critical thruster in terms of exceeding its lifetime. As currently projected, the PIA thruster would need to execute ≈27,000 thruster pulses to perform the mission as planned. This may be reduced by biasing the trajectory to decrease the likelihood POSZ clean-up maneuvers or by utilizing Z-thrusters for precession maneuvers (either implementation offers propellant savings as well). However, the current 23,000 pulse limit is expected to be increased to 35,000 in the near future, due to further ground test work performed by the engine manufacturer.[9] In summary, it appears that the lifetime concerns related to thruster cycles will be alleviated in the near future.

VIII. 10-N Thruster TCM Summary

Between launch in October of 1989 and the end of year 1992, a total of seventeen 10-N trajectory correction maneuvers (TCMs) were executed on the spacecraft. Three potential TCMS were canceled due to excellent spacecraft navigation: the final

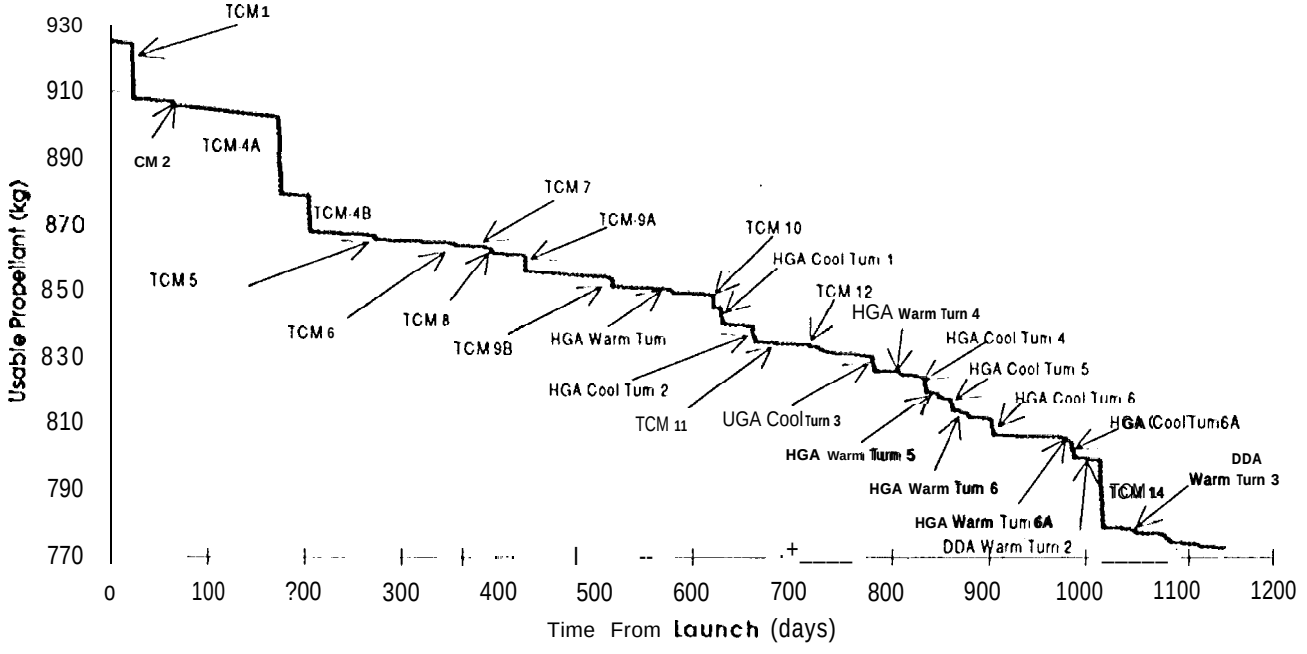

Figure 15, Galileo Usable Propellant History

Table 5. RPM Consumable Summary as of EOY 1992

RPM Consumables	Used	Lifetime	% Used
21A, 72A Thruster Valves (cycles)	1861	23000	8.09%
21 B, Z2B Thruster Valves (cycles)	1362	23000	5.92%
PIA Thruster Valve (cycles)	9206	23000	40.03%
P2A Thruster Valve (cycles)	8820	23000	38.35%
L1 B, L2B Thruster Valves (cycles)	9646	23000	41.94%
SIA Thruster Valve (cycles)	178	23000	0.77%
SIB Thruster Valve (cycles)	120	23000	0.52%
S2A Thruster Valve (cycles)	158	23000	0.69%
S2B Thruster Valve (cycles)	120	23000	0.52%
B-branch Latch Valves (cycles)	377	4000	9.43%
A-branch Latch Valves (cycles)	687	4000	17.18%
400-N Latch Valves (cycles)	1	4000	0.03%
Oxidizer (kg NTO)	92.27	571.3	16.15"4
Fuel (kg MMH)	60.42	353.87	17.07%
Total Propellant (kg)	152.68	925.17	16.500/!
Propellant Usage Breakdown (kg)			
TCMs	88.51		57.97%
HGA Anomaly Activity	44.97		29.45%
Attitude Control	15.95		10.44%
RPM Maintenance	3.27		2.14%

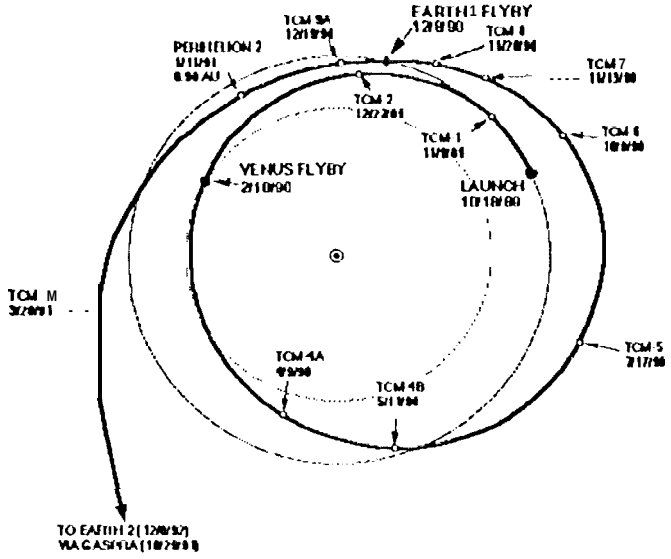

Figure 16. Galileo TCMs: Launch to Earth-1

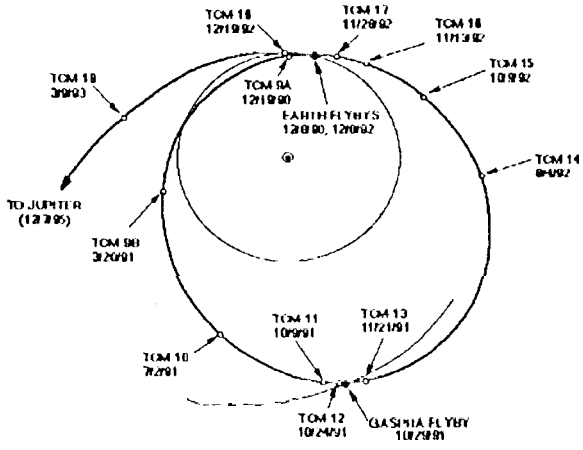

Figure 17. Galileo TCMs: Earth-1 to Earth-2

Venus targeting maneuver (TCM-3, January 1990), the post-Gaspra clean-up maneuver (TCM-13, November 1991), and the post-Earth-2 clean-up maneuver (TCM-18, December 1992). Despite occasional unexplained shifts in thruster performance (discussed in depth below), all seventeen Galileo TCMS to date have been executed well within requirements. Figure 16 shows the heliocentric trajectory of Galileo between launch and the first Earth flyby, with the locations of the trajectory correction maneuvers labeled. Figure 17 represents an analogous plot for the Earth-1 to Earth-2 trajectory leg.

TCM-1 was performed in three portions (days) and was a largely deterministic maneuver, to remove the planned launch bias imparted by the IUS. TCM-1 executed nominally, with the exception of the previously mentioned 21A thruster temperature transducer failure. The overburn from TCM-1 necessitated a POSZ component for TCM-2; although performing POSZ trajectory correction is not desirable (due to inefficiency), the RPM performance during TCM-2 was well within specifications. In fact, an excellent Venus gravity assist was obtained February 10, 1990, without any additional trajectory modifications.

TCM-4 was a large, deterministic maneuver utilized to "Patch" the launch/Venus trajectory to the Venus/Earth-1 trajectory. It was divided into TCM-4A and TCM-4B due to its large size. Both TCMS executed nominally, with two exceptions. The L2B thruster temperature sensor failed during TCM-4A, and the lateral thruster performance level shifted throughout the maneuver. This caused a small underburn during both TCM-4A and TCM-4B. However, errors were still well within requirements. TCMS 5 through 8 were used to successively target to the Earth-1 encounter aimpoint. This step-by-step targeting was required by Earth-avoidance constraints. These four TCMS executed very successfully, and the Earth-1 gravity assist was obtained December 8,1990.

TCM-9A and TCM-9B were provided to correct any Earth-1 delivery errors and to begin targeting to the asteroid Gaspra. Both of these maneuvers performed very well. TCM-10 targeted to the final Gaspra flyby aimpoint. It also had the distinction of being the first TCM performed as a 'turn-burn-

unwind' maneuver. This implementation saved 2.0 kg of propellant vs. a vector mode implementation of the same maneuver. TCM-11 and 1 CM-12 were purely statistical maneuvers to obtain the best possible Gaspra encounter. The largest uncertainty in the Gaspra flyby parameters was the position of Gaspra itself. The Gaspra ephemeris was improved greatly shortly before closest approach by utilizing optical navigation techniques with the Galileo SSI camera.[10] During the optical navigation campaign, exposures of Gaspra with stars in the background were taken. The excellent TCM-11 and TCM-12 execution employing this information facilitated the first ever reconnaissance by a spacecraft of a main-belt asteroid on October 29, 1991. Incidentally, optical navigation will be an essential part of the Ida flyby in August 1993 and for navigation during the Jovian orbital tour (using optical navigation of the four large Galilean moons to further refine their ephemerides). The scheduled post-Gaspra clean-up maneuver TCM-13 was unnecessary.

TCM-14 was executed in August of 1992 to shift from the Earth/Gaspra trajectory to the Gaspra/Earth trajectory. L-thruster performance variations again were prevalent, after a period of relative stability between TCM-4B and TCM-12. However, the overall maneuver accuracy of 1.3% was well within requirements. As with TCM-4A and TCM-4B, TCM-14 did not target to the final Earth-2 aimpoint, due to Earth-avoidance constrains. TCMS 15 and 16 each shifted the S/C closer to the final Earth-2 aim point. TCM-16 targeted directly to the final Earth-2 aimpoint at an altitude of 304 km. Both TCMS performed very well. Finally, TCM-I 7, another purely statistical maneuver, was executed to remove the TCM-16 delivery errors. Navigation and TCM-17 execution was so accurate that the planned post-Earth-2 clean-up maneuver TCM-18 proved unnecessary.

For trajectory correction maneuvers, the best estimate for maneuver performance is obtained from the Galileo Navigation Team's Orbit Determination (OD) solution following a maneuver. Table 6 summarizes the TCM performance delivery accuracy throughout the mission to date. The values of ΔV displayed in the fourth and fifth columns represent the designed values for the necessary spacecraft velocity increment in the axial and lateral directions, respectively. The next two columns were obtained from OD solutions and represent the executed maneuver accuracy ($\Delta V_{executed} / \Delta V_{designed} - 1$) during the axial and lateral components, respectively, of each maneuver. A summary of the TCM accuracy to date is provided at the bottom of Table 6. Notice that the overall maneuver performance average is +0.2%, very close to zero. Also, the demonstrated maneuver accuracy of ± 1.29'. (one sigma) is well within requirements. Indeed, this standard deviation has decreased somewhat, due to better characterization of the RPM system. The first four TCMS (I CM-l, TCM-2, TCM-4A, and TCM-4B) had the four largest average execution errors of all TCMS in this period of time. However, although a learning curve is apparent, fairly large errors continue to be observed. For example, the reasonably large error during TCM-14 is related to relatively large shifts in lateral thruster performance. This will be discussed in detail in the next section.

IX. 10-N Thruster Performance

Lateral Maneuvers -- L-Thrusters

All TCMS from launch to the end of 1992 have employed the L-thrusters, making them the most used thrusters to date. The lateral maneuvers, like all 10 N-thruster AV maneuvers, are broken down into several pulse trains called segments. A lateral maneuver is carried out in dual-spin mode. One L-thruster fires for about one second, and half a S/C revolution later, the other L-thruster fires, pushing the S/C inertially almost in the same direction. The direction is only approximate since the L-thrusters are cant-angled by 10 degrees from the S/C equatorial plane (so they can be used as backup precession thrusters). Due to the cant angle, each firing turns the S/C's angular momentum vector (or spin axis) by a small amount and also applies a tiny delta-V perpendicular to the desired AV direction (along the S/C 2-axis). The two L-thrusters are angled in an opposite fashion so that these undesired effects almost cancel out. However, only one of these two side effects can be zeroed out in the maneuver design. The ground software (S/W) is built to minimize the spin axis turn angle (also called attitude excursion). The uncompensated AV component along the Z-axis has to be accounted for by navigation in the trajectory design. The minimization of the spin axis precession specifies that the pulse on-times for the L1 B-thruster are longer than for the L2B-thruster, because their effective moment arms are different (i.e., the center of gravity is not in the center of the RPM thruster cluster booms). Typically the on-times are 1.3s for L1 B thruster and 0.94 s for L2B thruster during lateral maneuvers.

It was noticed via real-time (R/1) Doppler observation very early in the mission that the impulse delivered by the thrusters changed through the course of a segment by about 1 % to 1.6°/0. A segment usually consists of about 100 to 150 pulses. This performance change was not a surprise since the propellant tank pressures decrease at the beginning of a maneuver until the regulator opens. In addition, the temperatures in the cluster rise. This causes the propellants to warm up before they reach the engine. 1 his effect is particularly evident in pulse-mode operation because the propellant dwell time in the warm cluster and the hot thruster valve is about 20s in each, versus about 1 s if continuous-mode firing were performed. This propellant pre-heating lowers the thrust by approximately 10/. through the course of an average segment.

The first large lateral maneuver, TCM-4A, was a so-

Table 6. TCM Summary Table

TCM	DATE (S)	MANEUVER DESCRIPTION	V(z) m/s	V(L) m/s	%ERR V(z)	%ERR V(L)	%ERR TOTAL
TCM-1	11/9/89-11/11/89	REMOVE LAUNCH BIAS & 1ST VENUS TARGET	15.6	1.74	+1.7	+3.5	+1.7
TCM-2	12/22/89	2ND & FINAL VENUS TARGET	0.16 POSZ	0.72	+2.2	+2.1	+2.1
TCM-4A	4/9/90-4/12/90	1ST EARTH-1 TARGET PART 1	----	24.7	---	-2.3	-2.3
TCM-4B	5/11/90-5/12/90	1ST EARTH-1 TARGET PART 2	-----	11.3	---	-2.4	-2.4
TCM-5	7/17/90	2ND EARTH-1 TARGET	0.72	0.59	+2.5	-0.2	+1.4
TCM-6	10/9/90	3RD EARTH-1 TARGET	0.48	0.20	+0.8	-1.6	+0.4
TCM-7	11/13/90	FINAL EARTH-1 TARGET	1.09	0.66	+1.2	+1.3	+1.2
TCM-8	11/28/90	TCM-7-CLEAN-UP TCM	-0.021 POSZ	0.05	+1.2	-0.6	-0.4
TCM-9A	12/19/90	POST EARTH-1 CLEAN-UP	----	5.29	---	-0.2	-0.2
TCM-9B	3/20/91	GASPRA TARGET PART 1	0.20 POSZ	2.27	+0.5	+0.6	+0.6
TCM-10	7/2./91	GASPRA TARGET PART 2	----	3.65	---	-0.9	-0.9
TCM-11	-10/9791	GASPRA TARGET CLEAN-UP TCM	0.09 POSZ	0.34	+0.4	+0.0	+0.0
TCM-12	10/24/91	GASPRA TARGET CLEAN-UP TCM	0.02	0.21	+0.6	+0.2	+0.2
TCM-14	8/4/92-8/7/92	1ST EARTH-2 TARGIST	0.41	21.0	+2.7	+1.3	+1.3
TCM-15	10/9/92	2ND EARTH-2 TARGET	0.40	0.61	+0.4	+0.8	+0.6
TCM-16	11/13/92	FINAL, EARTH-2 TARGET	----	0.89	---	-0.5	-0.5
TCM-17	11/28/92	EARTH-2 TARGET CLEAN-UP TCM	0.02	0.02	+0.0	+0.0	+0.0

AVERAGE MANEUVER EXECUTION ERROR	= +0.2% = +0.2%
STANDARD DEVIATION	= ±1.2% ±1.2%
DEMONSTRATED 3 SIGMA DELIVERY	= -3.4% TO +3.8% ±3.8%

called multi-portion maneuver. It stretched over four days (portions), six segments per day, about 130 pulses per segment. At the beginning of days 2, 3, and 4, the cluster and tank temperatures as well as the tank pressures were almost identical. The impulse, however, observed through the Doppler measurement indicated a drop of about 0.5% from day to day. This change of AV performance was accompanied by unexpectedly large attitude excursions,

The drop in ΔV performance as well as the attitude excursions continued in the same fashion through the first portion of TCM-4B. From the second portion of TCM-4B through TCM-12 (except for TCM-6), the AV performance was steady, within ±0.5% (see "diamond" markers in Figure 18); however, attitude excursions were evident during mostofthese maneuvers.

The attitude excursion is a function of the difference of the y-torque delivered by the L1B thruster and the y-torque applied by the L2B thruster. The difference in these torques corresponds directly to a difference in the impulse-bits delivered by each of the L-thrusters, if the change in moment arms over the course of one maneuver due to small shifts of the center of gravity is neglected (which is a valid assumption). The achieved AV is a function of the sum of the two impulse-bits. Both pieces of information together allow an estimate of the net thrust provided by each individual L-thruster. It appears that the LIB-thruster was mainly responsible forthe observed large attitude excursions and the decline in the ΔV performance (see hick, solid line in Figure 18). From TCM-5

through TCM-8, the attitude excursions were very small or even zero, because the thrust ratio in the design of the maneuver was chosen very accurately. Note that if the thrust ratio chosen in the design of the maneuver (lower solid thick line in Figure 19) matches exactfy the real thruster performance on-board during the maneuver (lower thin line), the attitude excursion is zero (upper solid line). If the real ratio is smaller than assumed in the design the attitude excursion becomes 'negative: the more the two differ the more excursion buildup is generated.

TCM-9B and TCM-10 were peculiar since the ΔV performance was close to nominal but at the same time they exhibited conspicuous attitude excursions. This means that the difference of the thrust magnitudes (or impulse-bits) of the two L-engines had changed while their sum stayed nearly the same,

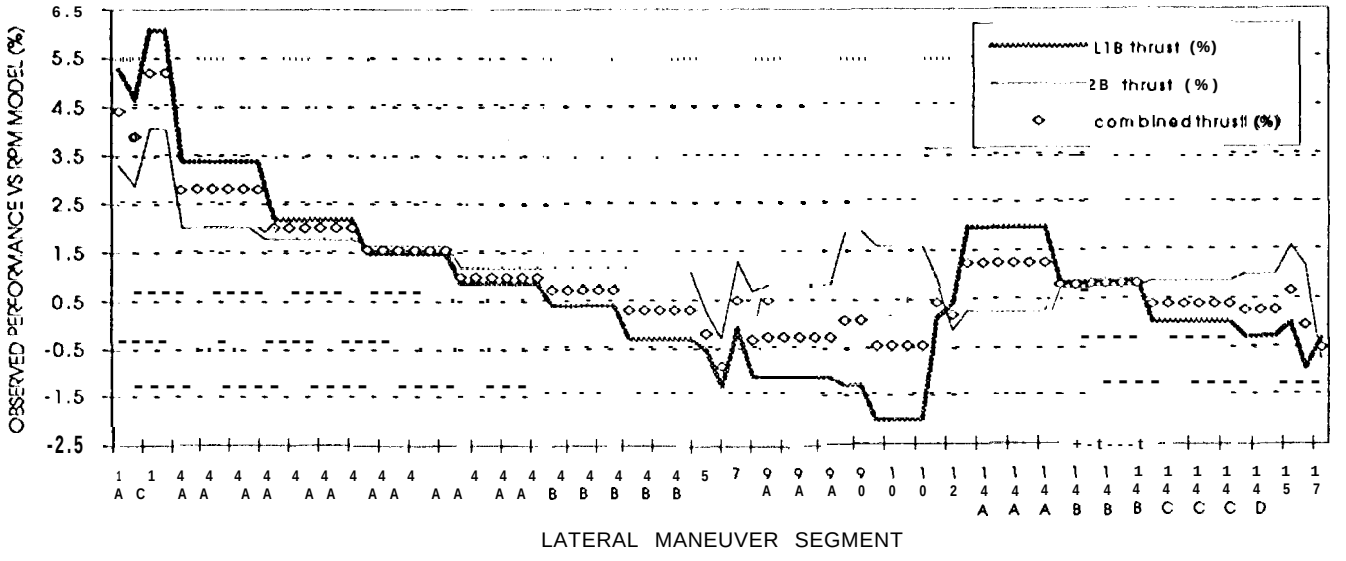

Figure 18. RPM TCM L-Thruster Performance

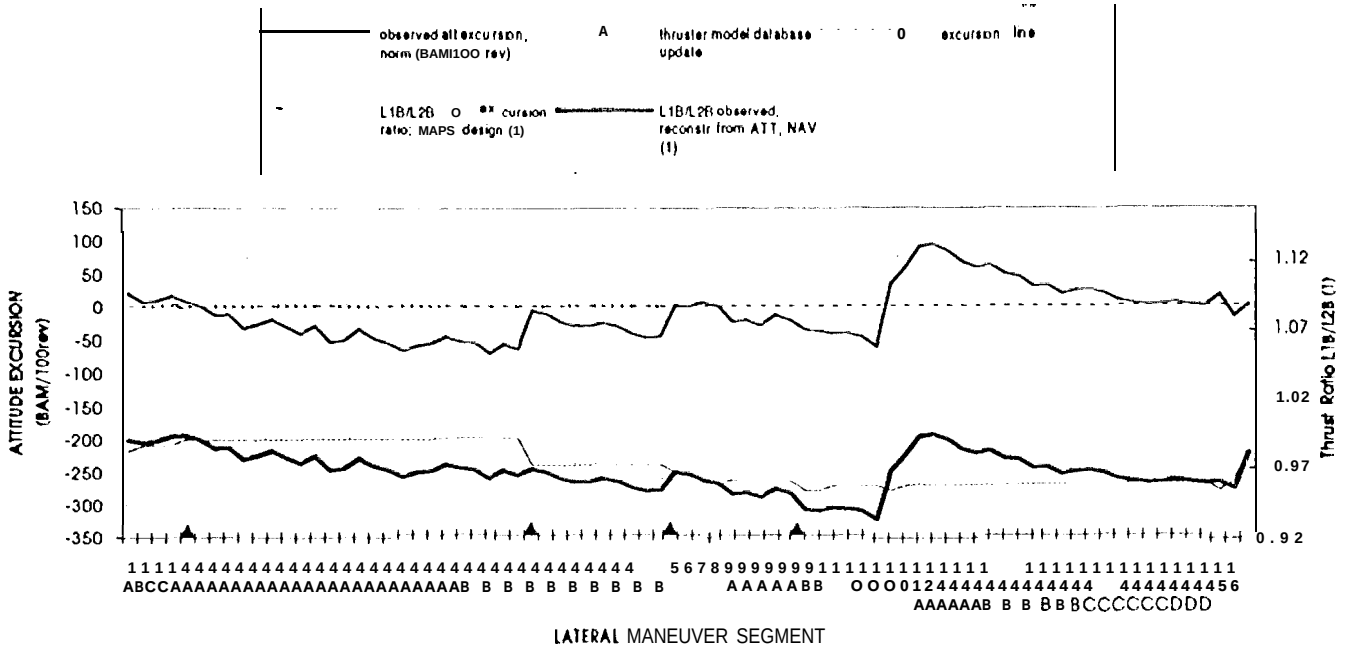

Figure 19. Galileo Attitude Perturbation During Lateral TCMs

suggesting an equal but opposite shift in the performance of the two L-thrusters.

Fundamentally the reconstruction revealed that the thrust ratio L1 B/L2B had steadily decreased between launch and TCM-10 (see lower solid line of Figure 19). If the thruster simulation models would not have been updated, the attitude excursion as well as the AV error would have become unacceptable.

This trend turned around radically during TCM-11, TCM-12 and the first segment of TCM-14. The thrust ratio recuperated during these three maneuvers back to where it was at the beginning of TCM-4A. In addition to the change in relative thrust ratio, the observed, combined thrust of both L-thrusters also increased by about 2% from the end of TCM-1 O to the beginning of TCM-14.

During TCM-14 the thrust ratio and the total thrust declined, just as they had between TCM-1 and TCM-10. The reason for this peculiar behavior, which seems to be almost completely attributable to the L 1 B thruster, is not understood at this time.

Positive Z-Maneuvers -- P1A-Thruster

There have been only five positive-Z maneuver segments, all using the P1A-thruster. The largest was in TCM-9B. This type of maneuver also showed (similar to other maneuvers) significant overperformance versus the Propulsion System Simulation Program (PSSP) reconstruction, which is based on the measured ground test performance. The discrepancy has not been explained satisfactorily to date. There was quite a discrepancy between the observation from the Doppler measurement and the solution from the orbit determination (OD) during T CM-2 (see Figure 20); later these two 'measurements" agree quite well. It appears that there is no trend in the thruster performance versus time. The overperformance recorded by Doppler measurements was 5.4±0.6% (la) and from the OD 3.7*1.40/0 (1σ). The PSSP model was adjusted by +5% prior to TCM-8 and since then the POSZ-TCM execution accuracies have been very good.

Pulsed Z-Maneuver (A-Branch) -- Z(A)-Thrusters

The first TCM started out using the A-branch Z-thrusters, -Z1 A and -22A. Eighteen segments (each about 100 pulses) were executed in two portions. After the thruster temperature transducer failed on -21A it was decided to switch to the B-branch for the last portion of TCM-1. Since that time, the B-branch has been the primary branch for PULZ type maneuvers since it exhibits almost no perturbations on the spin rate. There was no usable Doppler

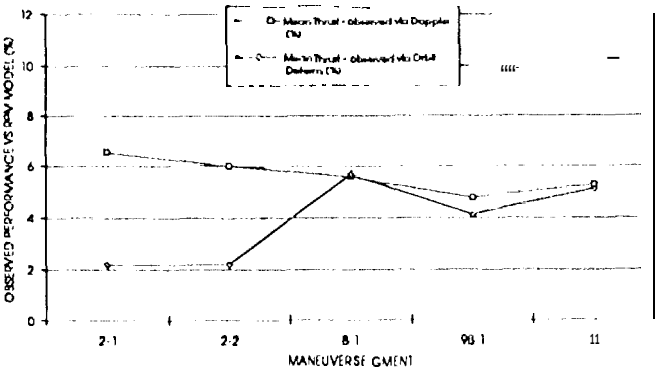

Figure 20. RPM POSZ TCM Performance

data available for the PULZ(A) maneuvers. The OD solution indicated a 0.7% overburn in the first portion and 0.9% during the second portion of TCM-1. This appears to be the lowest overperformance observed on the Galileo 10 N-thrusters.

Pulsed Z-Maneuvers (B-Branch) -- Z(B)-Thrusters

There have been fourteen pulsed -Z (PULZ) maneuver segments using the B-branch Z-thrusters, -Z1B and -Z2B. Figure 21 shows the observed performance levels of these maneuvers versus the PSSP reconstruction, which uses the telemetered tank pressures and propellant temperatures as an input. During TCM-1 there was quite a "noisy" Doppler measurement compared to the reconstruction. This was caused by an unfavorable Doppler look angle of 91.8°. Since TCM-5 there has been good agreement between the Doppler measurement and the OD solution. The average AV weighted overperformance for the maneuvers since TCM-5 is 2.0±0.3%(1σ) derived from OD and 1.9±0.1%(1σ) observed by Doppler. The model was updated by raising the performance of both thrusters by 1.6% prior to TCM-6 and again to +2.0% prior to TCM-7 with excellent results in the PULZ-TCM execution since.

S-Thrusters

The S-thrusters are not used very often, except for tiny spin correction maneuvers and flushing maneuvers. During these maneuvers they fire two pulses with approximately one second on-times. Thirteen earfy flushing maneuvers were analyzed. The observed performance ranged from 3.40/. to 5.5% higher than expected. The +S2A thruster showed an overperformance of 3.4±1 .2% (la), while the +S2B thruster exhibited 3.6±1.1%(1σ) overperformance. The overperformance on the -S1 A thruster was 5.5%±0.9%(1σ) and 3.6±1.0% (1σ) was observed on the -S1 B thruster.

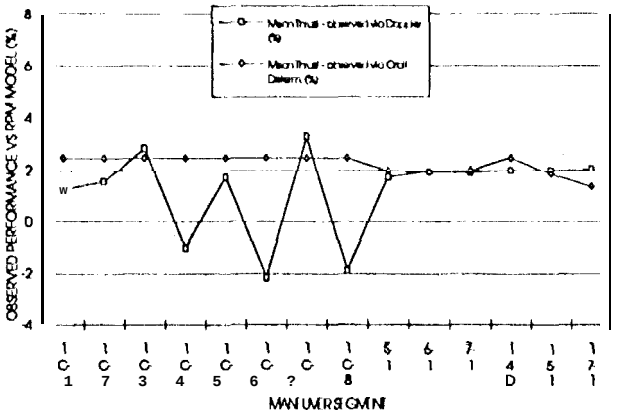

Figure 21. RPM B-branch PULZ TCM Performance

Table 7 represents the best estimate for the thruster performance during all analyzed 1O-N thruster activities. Performance estimates of the Galileo 10-N thrusters are vital to characterize the engines, since maneuver firing durations are determined a priori (i.e., they are not governed by accelerometer cut-off). The one-sigma errors stated in the table (like in the section above) reflect the calculated standard deviation from the different maneuver reconstructions. For this reason, the performance deviation for unbalanced turns and A-branch PULZ maneuvers is only 0.1%, since there are only two data points in each case. Certainly the true uncertainty on the performance value is larger than this. Also keep in mind that the same thruster may perform differently for a different maneuver types, because misalignment or plume impingement mismodeling may favor the thrust level in one direction but diminish it in another. This is because Galileo is a dual-spinning spacecraft and thus the thrusters interact differently with the spacecraft depending on the relative orientation of the thrusters with the despun section,

Table 7. RPM IO-N Thruster Performance Summary

Maneuver Type	Thruster	Best Estimate of Real Performance vs. Model (±1σ)
LAT(B)	L1B	0.7±1.8%
	L2B	0.7±0.8%
POSZ(A)	P1A	4.5±0.7%
BAL. TURN(A)	P1A&P2A	6.5±3.0%
UNBAL. TURN (A)	Z1A&Z2A	3.0±0.1%
PULZ(A)	Z1A&Z2A	0.8±0.1%
PULZ(B)	Z1B&Z2B	2.0±0.3%
SPIN(A)	S2A	3.4±1.2%
SPIN(B)	S1 A	5.5±0.9%
	S2B	3.6±1.1%
	S1B	3.6±1.0%

Thruster Performance During AACS Maneuvers

During the Galileo mission, over 160 spacecraft precession maneuvers have been executed, The vast majority of spacecraft turns have been executed using the PIA and P2A thrusters (balanced or quasi-balanced maneuvers). However, some unbalanced turns using the Z1 A and 22A thrusters have been executed as well. Unbalanced turns may complicate mission navigation, since non-negligible velocity changes are added to the spacecraft at arbitrary points of the trajectory. However, the ≈65% propellant savings of unbalanced turns (due to the larger moment arm of the Z-thrusters) more than compensates for the additional complication to navigation. Spacecraft turns were performed for a variety of reasons, including Earth-pointing for telecommunication, sun-pointing thermal constraints, attitude adjustment for turn-burn-unwind TCMs, and for solar thermal perturbation during HGA rib release attempts.

P-Thruster Turns

The performance of the P-thruster couple or Z-thrusters during spacecraft turns may be determined from RPM and AACS data. Unlike TCMs, spacecraft turn maneuvers do not fire a fixed number of thruster pulses. Rather, an AACS control algorithm ceases thruster firings when the correct spacecraft attitude has been obtained. Therefore, a thruster overperformance would show up as a reduced number of thruster pulses, not as an overshoot of the targeted inertial attitude. The average thrust of the P-thruster couple or Z-thrusters maybe determined by examining the attitude change of the spacecraft during the maneuver, together with the relevant spacecraft properties (e.g., spin rate and rotor moment of inertia). This observed thrust for the thruster couple may be compared with the modeled thrust level for the couple to determine the relative performance of the thruster pair. It should be mentioned that the individual performance of each P-thruster or Z-thruster is not discernible from this process.

Over 150 P-thruster maneuvers were analyzed to determine the performance of the P-thruster couple vs. ground test levels. It was determined that the P-thruster couple overperformed by an average level of +6.5% vs. pre-launch levels. It seems that the P-thrusters are overperforming more than any of the other 10-N thrusters. Moreover, the average performance level has shifted very little (< 0.2%) throughout the mission, in contrast with the L-thruster performance shift (≈7.5%). When the performance of each P-thruster turn was plotted vs. accumulated firing time, the data clustered around the average value of +6.5%, but the standard deviation was high (3.0%). However, if the P-thruster performance is viewed as a function of the executed turn angle of precession, large deviations from the average performance value of +6.5% only occur for small turns (see Figure 22). Specifically, for turns

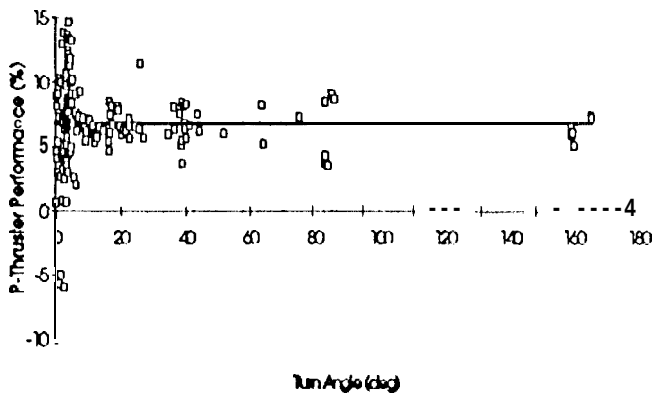

Figure 22. RPM P-Thruster Precession Maneuver Performance

larger than 5°, the standard deviation is only 1.8%. It should be pointed out that one reason the P-thruster performance may appear so high is because the modeled plume impingement loss for the P-thruster couple of 2.1% maybe overfy pessimistic. Other thrusters have modeled plume impingement losses from 0.5% to 1%. This result may seem somewhat counterintuitive and warrants some discussion. The P-thrusters have overperformed vs. unplumed ground models by +4.4%. Hence, with a 2.1% modeled plume impingement loss, the actual P-thruster performance must have been +6.5% vs. plumed ground models. Since the +4.4% performance is independent of plume effects, a reduced modeled plume impingement value would result in lower actual P-thruster overperformance.

This high overperformance of the P-thruster couple is corroborated somewhat by the inferred performance of the PI A thruster during POSZ TCMs. In particular, the PI A thruster overperformed by an average of +4.5% vs. ground test levels in POSZ TCMs. No other thruster has averaged as high of an overperformance during TCMs. The inconsistency of the PI A POSZ TCM result and the P-thruster couple performance result cannot be explained by assuming that the P2A thruster is overperforming by roughly 8.5%. This is because the Galileo Navigation team has determined that the P1 A thruster is overperforming more than the P2A thruster during precession maneuvers from the minute AV imparted to the spacecraft during balanced turns, measurable through the Doppler shift. However, thruster misalignments and uncertainties in the precession maneuver analysis are probably sufficient to explain the discrepancy.

Z-Thruster Turns

Through the end of 1992, only two unbalanced turns had been executed on the Galileo spacecraft. A demonstration of the unbalanced turn capability was performed in early 1991, using the Z1A and 22A thrusters to execute a 7° spacecraft turn. The turn executed highly successfully, with less spin and pointing excursions than encountered during balanced turns. An examination analogous to the one mentioned above was performed to determine the relative A-branch Z-thruster performance level during the unbalanced turn. A +3.1% overperformance above the ground-test level was noted.

In July 1992, a second unbalanced turn maneuver was performed in support of the DDA2 activity mentioned previously. T his turn was much more substantial--the spacecraft was turned through an angle of ≈30°. Again, spin and pointing performance was excellent, and the performance level of the Z-thruster couple was determined to be +2.9%. It appears that A-branch Z-thruster performance during unbalanced turns is quite repeatable; however, this observation is made with only two data points.

Other performance data is available on the A-branch Z-thrusters from PULZ maneuvers during T CM-1. From maneuver reconstruction, the A-branch Z-thrusters overperformed during TCM-1 by 0.8% vs. pre-launch levels. This is somewhat lower than the performance value inferred for unbalanced turns. The discrepancy may be explained by the different operating mode of the two maneuver types. In a PULZ TCM, each Z-thruster fires twice per revolution, while the 21A and 22A thruster only fire once per revolution for unbalanced turns. The performance difference may be due to differences in plume impingement between the two sides of the spacecraft at which the Z-thrusters are fired, or differences in thruster moment arms.

X. RPM Helium Budget and Regulator Operation

The RPM Analysis Team tracks the total helium mass on the spacecraft as a function of time. This total should remain nearly constant, since only 40 grams of helium out of ≈2700 grams loaded is dissolved in the propellants and expelled along with them during maneuvers. Nominally, helium should just shift from the pressurant tanks to the propellant tanks during periods of pressure regulation. Therefore, since the amount of helium in each tank is calculable from spacecraft telemetry and the book-kept propellant masses in the tanks, the total may be added up to verify that it is invariant. This so called “helium budget” offers an independent check of the health of the propulsion system (particularly with regard to possible helium or propellant leakages). Figure 23 represents a typical plot of the helium budget. The bottom curve represents the helium in the pressurant tanks; the top curve is the total helium. Notice that the helium in the pressurant tank is quite ‘noisy”--this is due to the coarse measurement of the helium tank pressure.

Figure 24 is an enlarged view of the middle curve of Figure 23. This curve represents the total helium on board minus

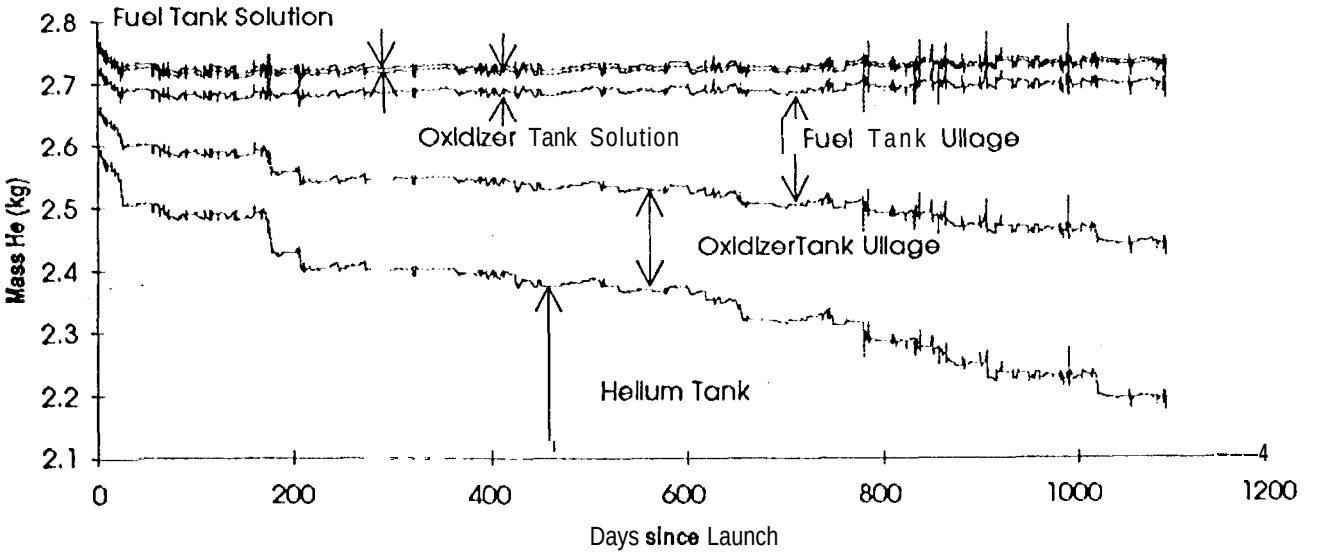

Figure 23. RPM Helium Budget

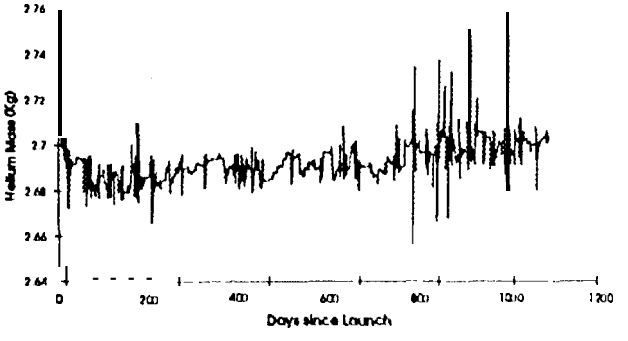

Figure 24. RPM Total Gaseous Helium Mass

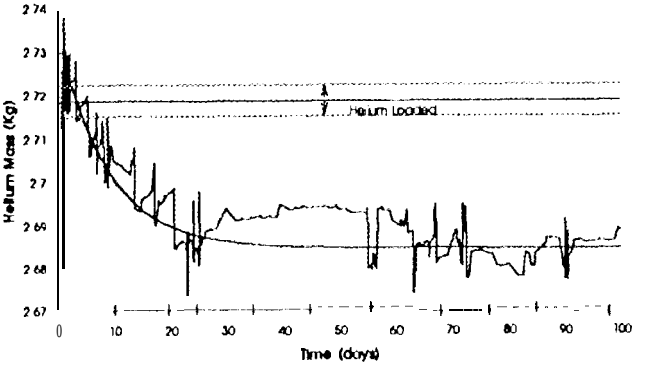

Figure 25. RPM Post-Launch Helium Volubility

the helium modeled in propellant solution. Although this curve should have remained constant, it actually appears to increase vs. time. This apparent increase could be explained by a systematic error in the propellant consumption model used by the RPM Analysis Team of 5.8%. This error seems too large. Considering the overperformance of the thrusters, it is very unlikely that the propellant consumption is lower than modeled because both observations would drive up the Isp of the 10-N engines by an unbelievable 10%. Therefore, it is likely that the helium tank pressure transducer has drifted upward. In Figure 25, the apparent overshoot and decay in the total helium mass during the first twenty to thirty days of the mission is quite significant. The decay of the curve in Figure 25 gives some information about the rate of helium volubility in propellants. A simple exponential best-fit curve was calculated from the data in Figure 25, to help characterize the time constant of the helium volubility. This time constant was found to be ≈9 days. The apparent overprediction of the helium mass following pressurization may be due to the calculation uncertainty in measuring the oxidizer and fuel tank pressures, since these tanks were loaded at low pressure (3 bar). The RPM best-estimate value for the total helium in total loaded NTO and MMH solution just after saturation is 44±7.3 grams (1σ).

The volubility rate is not simply a function of chemistry and physical tank variables. In particular, spacecraft accelerations (e.g., from maneuvers) or temperature fluctuations may cause earlier saturation of the pressurant gas than anticipated here. The first Galileo TCM was performed on day 22 of the mission. Notice from Figure 25 that equilibrium had more or less been obtained by that time, so TCM-1 dynamics did not influence the Galileo helium volubility rates. However, some small Galileo propulsive maneuvers (e.g., sun acquisitions and flushing maneuvers) were performed before TCM-1. Their influence on the helium volubility rates are unknown, but should be minor.

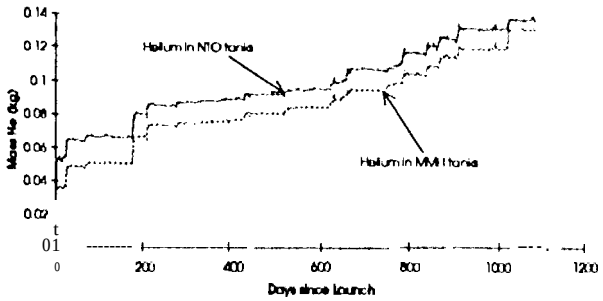

Figure 26. RPM Total Helium Mass in MMH and NTO Tanks

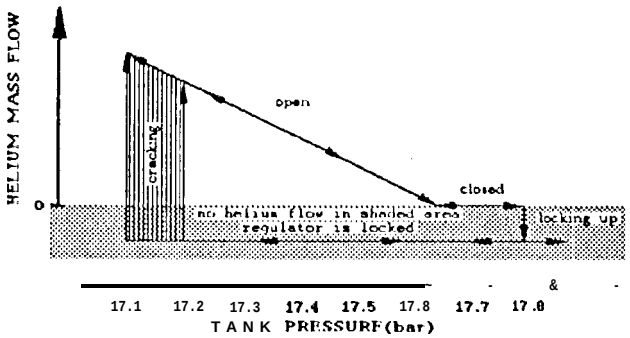

Figure 27. RPM Pressure Regulator Operation

An additional insight available from a helium budget is the best knowledge of the pressure regulator history. Figure 26 displays the total helium mass in the oxidizer and fuel tanks as a function of time. As expected, the output is much less noisy than the curves of Figure 23, since the primary error source in the helium budget is the knowledge of pressurant tank helium pressure. A number of regulator openings, or trackings, may be discerned from the figure. The increases in helium around mission days 25,65,170, and 210 correspond to TCM-1, TCM-2, TCM-4A, and TCM-4B, respectively. The slow rise in helium mass evident between mission days 260 and 430 represent a fine regulation of helium by the pressure regulator following a 'weak regulator cracking." Many of the regulator trackings between mission days 700 and 1000 represent HGA deployment activities, usually 165° HGA Cooling Turns. The large regulator cracking around mission day 1025 corresponds to TCM-14, the second-largest maneuver (AV ≈ 21 m/s) performed to date. To conclude, plots such as Figure 23, together with propellant tank pressure data, offer the best chance to analyze the sixteen or so regulator trackings that occurred since launch. Although the regulator operation has not boon analyzed in great detail, enough data has been examined to allow the RPM Analysis Team to say that the soft-seat pressure regulator has performed excellently through three years of mission operations.

Some aspects of the interactive regulator and check valve operation were not anticipated prior to launch. The ground tests, which were focused only on verifying the specifications of each component, did not sufficiently characterize the exact regulator and check valve interactive behavior.

First it was discovered that there is quite a hysteresis between the lockup pressure (at almost 17.8 bar downstream of the check valves) and the cracking pressure, which is 0.6 to 0.7 bar below that. Whenever the tank pressures get thermally driven over the lockup pressure level, the regulator does not open again until a propellant expulsion or temperature decrease has lowered the tank pressures (usually below 17.2 bar). Prior to launch it was assumed that the regulator together with the check valves would re-open at about 0.2 bar below the lockup. The observed operation of the regulator/check valve combination is actually more desirable in mission operation, because it allows tank temperature decreases without immediate recharging of the tanks with pressurant (ratcheting), which then would limit the range of subsequent tank temperature increases (dictated by the tank pressure limit of 18.5 bar).

The second observation of regulator operation was its excellent regulation ability at exceedingly low flow rates. Once open, it regulated the tank pressures at an almost constant level (about 0.15 bar below lockup pressure) for many months. It opened and closed many times (fine regulation) during that time but it never really locked up. It was not until a tank temperature increase raised the tank pressure that the regulator locked, As graphically shown in Figure 27 the regulator does close at about 17.65 bar and the pressure can only be further increased through tank temperature increase to achieve a true lockup. The characteristic behavior that regulator trackings (after true lockups) occur 0.6 to 0.7 bar below the lockup pressure can only be observed if a thermal back pressure is applied to the check valves and/or the regulator. This was not done in ground testing; therefore, this was not expected. But again the observed regulator/check valve behavior is more convenient for mission operations than the one anticipated pre-launch.

XI. Conclusions

The Galileo RetroPropulsion Module (RPM) has performed excellently throughout over three years of flight operations. All 10-N thrusters have operated within requirements, and the Galileo navigation has been superb. The EOM propellant margin, defined at the ninetieth percent confidence level for ten satellite encounters in the Jovian system, has improved from -58 kg at launch to -3 kg (for the two asteroid encounter option).

Very few anomalies have occurred in the RPM through the end of 1992. A total of four of the twelve 10-N thruster

temperature transducers have failed open circuit. This has no operational impact on the RPM Team, since cluster temperature measurements adequately characterize the 10-N thruster behavior. Some unexplained shifts in lateral thruster performance have been observed. However, TCM delivery accuracy has still been very good overall.

The pressure regulator has worked excellently throughout mission operations. Between launch in October, 1989 and the end of 1992, approximately sixteen nominal regulator openings took place. After true lockups, regulator trackings have occurred 0.6 to 0.7 bar below the lockup pressure. This was not anticipated, since thermal back pressure was not applied in ground testing. A calculated helium mass budget for the RPM has demonstrated that there are no discernible external or internal helium leaks. Some volubility data was obtained for helium in nitrogen tetroxide following the initial pressurization of the RPM post-launch.

10-N thruster performance has generally been 1?'. to 7°/0 higher than the best estimate for the ground-test thrust levels. Performance data has been obtained from Trajectory Correction Maneuvers (TCMs), as well as from spacecraft precession and spin-correction maneuvers. No permanent degradation in thruster performance has been detected.

The Galileo High Gain Antenna (HGA) deployment efforts throughout the mission to date have brought special challenges to the RPM. Extended durations at large off-sun attitudes and low solar distances, executed for HGA tower and/or HGA deployment motor assembly warming/cooling, have perturbed the normally quiescent thermal state of all RPM components. However, these unplanned mission events have allowed further thermal characterization of the RPM than would have otherwise been possible.

Acknowledgments

The research described in this paper was carried out by the Jet Propulsion Laboratory, California Institute of Technology and the German Space Operations Center (GSOC), under contracts with the National Aeronautics and Space Administration (NASA) and the Federal Republic of Germany (FRG) Bundesrninister für Forsshung und Technologies (BMFT), respectively. The authors wish to acknowledge the following individuals who contributed to this research: Richard Cowley, Phil Garrison, Laura Grondalski, Cart Guernsey, Charlie Jennings, Hartwell Long, and Jeff Weiss. The authors would like to gratefully acknowledge the contributions of Robert Shotwell who helped bring this paper to fruition.

Dedication

Mr. Barber and Mr. Krug wish to dedicate this paper to Bernard M. Froidevaux, whose memory lives on following his untimely passing on March 5, 1993. His contributions and friendship will not be soon forgotten.

References

1. D'Amario, Louis A.; Bright, Larry E.; Bymes, Dennis V.; Johannesen, Jennie R.; and Ludwinski, Jan M.: "Galileo 1989 VEEGA Mission Description," AAS Paper 89-431, August, 1989.

2. Diaz, Af; and Casani, John R.: 'Galileo on Track to Jupiter," Astronautics & Aeronautics, February, 1983.

3. Jones, C. P.; and Landano, M. R.: 'The Galileo Spacecraft System Design," AIAA Paper 83-0097, January, 1983.

4. Bohnhoff, K., "Retro Propulsion Module (RPM) Bipropellant Unified System for Galileo,"' IAF Paper 82-326, September, 1982.

5. Immich, H.; I-angel, G.; and Munding, G.: 'Satellite Unified Bipropellant Propulsion System Experiences and improvements,' AIAA Paper 89-2506, July, 1989.

6. Cole, ?. W.; Frisbee, R. H.; and Yavrouian, A. H.: 'Analysis of Flow Decay Potential on Galileo," AfAA Paper 87-2016, June, 1987.

7. O'Neil, William J., 'Project Galileo Mission Status,' IAF Paper 91-468, October, 1991.

8. Kühne, J. F. W., 'Galileo - RPM Updated 1O-N Thruster Performance Model (Based on S/N 16 - May 1991 Tests)," DASA Document RPM-PN1500-92-01A, October, 1992.

9. Gotzig, "Galileo Test Report for 10N Thruster SN 16 Pulse Performance, Low Temperature Start-Up and Delta Life Tests,"' DASA Document RPM-TR1500-91-16, July, 1992.

10. Kallemeyn, P. H.; Haw, R. J.; Pollmeier, V. M.; and Nicholson, F. T.: "Galileo Orbit Determination for the Gaspra Asteroid Encounter," AIAA Paper 92-4523, August, 1992.